Available online at www.sciencedirect.com
ScienceDirect
Advances in Mathematics 223 (2010) 2166–2199
ADVANCES IN Mathematics
www.elsevier.com/locate/aim

Associahedra, cyclohedra and a topological solution to the A_∞ Deligne conjecture

Ralph M. Kaufmann [a,*], R. Schwell [b]

[a] *Purdue University, Department of Mathematics, 150 N. University St., West Lafayette, IN 47907-2067, United States*
[b] *Central Connecticut State University, Department of Mathematical Sciences, 1615 Stanley Street, New Britain, CT 06050, United States*

Received 4 January 2008; accepted 2 November 2009

Available online 4 December 2009

Communicated by Mark Hovey

Abstract

We give a topological solution to the A_∞ Deligne conjecture using associahedra and cyclohedra. To this end, we construct three CW complexes whose cells are indexed by products of polytopes. Giving new explicit realizations of the polytopes in terms of different types of trees, we are able to show that the CW complexes are cell models for the little discs. The cellular chains of one complex in particular, which is built out of associahedra and cyclohedra, naturally act on the Hochschild cochains of an A_∞ algebra yielding an explicit, topological and minimal solution to the A_∞ Deligne conjecture.

Along the way we obtain new results about the cyclohedra, such as new decompositions into products of cubes and simplices, which can be used to realize them via a new iterated blow-up construction.

Keywords: Operads; Deligne's conjecture; Actions on Hochschild complexes; Homotopy algebras; Polytopes; Cyclohedra; Associahedra; Little discs

0. Introduction

In the last years Deligne's conjecture has been a continued source of inspiration. The original conjecture states that there is a chain model of the little discs operad that acts on the Hochschild cochains of an associative algebra, which induces the known Gerstenhaber structure [9] on coho-

* Corresponding author.
E-mail addresses: rkaufman@math.purdue.edu (R.M. Kaufmann), schwellrac@ccsu.edu (R. Schwell).

0001-8708/$ – see front matter
doi:10.1016/j.aim.2009.11.001

mology. It has by now found many proofs [21,31,24,32,22,25,2,15], which all have their unique flavors. This plethora of approaches comes from the freedom of choice of the chain model for the little discs operad. Among these there are "minimal" choices which are cellular and have exactly the cells one needs to give the relevant operations induced by the operadic structure [24,25,15]. In the A_∞ algebra setting, where one only assumes that the algebra is homotopy associative, astonishingly there has so far been only one solution [22] based on homological algebra, although this subject is of high current interest for instance in Mirror-Symmetry, the theory of D-branes and String Topology.

In this paper, we give a new topological, explicit, polytopical, "minimal" solution via a cell model for the chains of the little discs which acts on the Hochschild complex of an A_∞ algebra. These cells are polytopical in the sense that they are products of associahedra and cyclohedra.

Theorem A *(Main Theorem). There is a cell model K^∞ for the little discs operad, whose operad of cellular chains acts on the Hochschild cochains of an A_∞ algebra inducing the standard operations of the homology of the little discs operad on the Hochschild cohomology of the algebra. Moreover this cell model is minimal in the sense that the cells correspond exactly to the natural operations obtained by concatenating functions and using the A_∞ structure maps.*

This statement is a statement over $\mathbb{Z}$.

Our construction can be viewed as a geometrization of a combinatorial operad $\mathcal{M}$ introduced by Kontsevich and Soibelman [22] dubbed the minimal operad. The operad $\mathcal{M}$ naturally acts on the Hochschild complex of an A_∞ algebra. In fact, it is the combinatorial distillate of the brace operations and A_∞ multiplications. Using polytopes, we construct a topological operad which has the homotopy type of a CW complex whose cellular chains form an operad isomorphic to $\mathcal{M}$.

First, we show that the differential of $\mathcal{M}$ is captured by the combinatorics of associahedra and cyclohedra. This allows us to construct a CW model K^∞ whose cellular chains are naturally isomorphic to $\mathcal{M}$. The proof that this cellular chain operad is a model of chains for the little discs operad is a bit involved. For this we need to compare three CW complexes, each built on polytopes. The first, K^1, is the cell model of the little discs which is the one given by normalized spineless cacti [15]; here the polytopes are just simplices. The second is the cell model K^∞ mentioned above; the cells in this complex are products of associahedra and cyclohedra. The last is K^{ht}, which is a mediating cell model constructed from trees with heights, where the cells are products of cubes and simplices. This model has a natural interpretation in terms of graphs of arcs on surfaces which define cell decompositions of moduli spaces of curves. The operad structure is closely related to the arc operad of [20], as we explain in detail in Appendix A.

We would like to emphasize that in contrast to the previous constructions of this type [15,17, 19]—which provided solutions to Deligne's conjecture, a cyclic version of Deligne's conjecture and moduli space operations respectively—the CW complexes provided by arcs in the present study *do not give the chain model that acts directly*. In the above contexts, the arc picture provided cells that could be directly used to define the action. Now, for the first time, we need to first consolidate the cells into bigger super-cells in order to have an action, as the original cells are too fine.

There is a chain of five propositions which leads to the Main Theorem:

Proposition I. *As chain operads $CC_*(K^\infty)$ and $\mathcal{M}$ are equivalent.*

Proposition II. *The cell models K^{ht} and K^{∞} have the same realization. Moreover, K^{ht} is just a cellular subdivision of K^{∞}.*

Proposition III. *The space $|K^1|$ is a strong deformation retract of $|K^{ht}|$.*

Proposition IV. *The map induced by the retract $r : |K^{\infty}| = |K^{ht}| \to |K^1|$ on the chain level, $r_* : CC_*(K^{\infty}) \to CC_*(K^1)$, is a morphism of operads. In fact, it is the map π_{∞} of* [15].

Proposition V. *(See [22].) $\mathcal{M}$ acts on the Hochschild complex of an A_{∞} algebra in the appropriate fashion; that is, it induces the Gerstenhaber structure on the Hochschild cohomology.*

The fact that $\mathcal{M}$ acts is true almost by definition; this is presumably why it is called the "minimal operad" in [22].

Proof of the Main Theorem. By Propositions I and V we see that $CC_*(K^{\infty})$ acts in the appropriate fashion. By Propositions II and III $|K^{\infty}|$ is homotopy equivalent to $|K^1|$ and since by [15] K^1 is a CW model for the little discs, so is K^{∞}. *A priori* this only has to be true on the space/topological level, but by Proposition IV on homology the retraction map r is an operadic isomorphism and hence K^{∞} is an operadic cell model. □

This actually answers a question of Kontsevich and Soibelman [22] about a smooth cell model for $\mathcal{M}$. In terms of a CW complex which is minimal in the above sense, it cannot be had. There is, however, a certain thickening of cells, which is indeed a smooth manifold model [18]. This is again given by a CW complex defined by trees, but with slightly different combinatorics. In this manifold model, the action on Hochschild is, however, not minimal; its dimension is already too big. It is nonetheless a very natural geometric realization and nicely linked to the arc complex and the arc operad of [20].

Our main tool for constructing the CW complexes is trees. In each case, we fix a particular combinatorial class of trees with a differential on the free Abelian group they generate. Based on this combinatorial data we build CW complexes, which are indexed by the particular type of tree such that the tree differential gives the gluing maps, and hence we obtain an isomorphism of Abelian groups between the cellular chains and the Abelian group of trees. The individual cells are assembled out of products of polytopes. These vary depending on the CW model we are constructing as mentioned above. The building blocks we use for K^1, K^{∞} and K^{ht} are, respectively, simplices, associahedra and cyclohedra, and simplices and cubes. The operad structures we consider are all induced from the topological level. In all three cases, pushing the operad structure to the homology yields an operad isomorphic to the homology of the little discs operad.

Theorem B. *The realizations $|K^{\infty}| \simeq |K^{ht}|$ and $|K^1|$ are all topological quasi-operads and sub-quasi-PROPs of the Sullivan-quasi-PROP $\mathcal{D}Sul^1$ of* [16]. *There is also a renormalized quasi-operad structure such that the induced quasi-operad structures on their cellular chains $CC_*(K^{\infty}) \simeq \mathbb{Z}\mathcal{T}_{\infty}$, $CC_*(K^{ht}) \simeq \mathbb{Z}\mathcal{T}_{ht}$, and $CC_*(K^1) \simeq \mathbb{Z}\mathcal{T}_{bipart}$ are operad structures and coincide with the combinatorial operad structure on the trees. Moreover, all of these operad structures are models for the little discs operad.*

The reader familiar with the constructions of [20] and [16] may appreciate that the gluings here are just tweakings of the usual gluings of foliations. In fact, as far as these structures are

concerned, the language of arcs on surfaces would be much easier. In the main text we phrase everything in the equivalent language of trees in lieu of that of arcs since it is a more widely-spoken language and the tree description is needed to define operations on the Hochschild complex. We will, however, provide a short dictionary in Appendix A and relegate the proof of Theorem B and Proposition I to this appendix as they are not absolutely essential to the argument of the Main Theorem. In this context, Proposition I can be replaced by the *ad hoc* Definition 3.6 (see Proposition 3.11).

Appendix A will be key in providing the A_∞ generalization of the results of [16,17] and will hopefully shed light on the different constructions stemming from string topology and mirror symmetry providing similar actions.

The realization that we need to consolidate the cells and the presented constructions are essential to the further study of chain level actions. One particularly interesting issue is the renormalization of the quasi-PROP composition. This is a novel feature that is necessary to obtain the correct combinatorics for the A_∞ case on the cell level. These cannot be handled by the arguments of [16] alone.

In the process of comparing the models, we establish new facts about the classical polytopes such as the cyclohedron, which are interesting in their own right.

Theorem C. *There is a new decomposition of the cyclohedron W_{n+1} into a simplex and cubes. Correspondingly, there is an iterated "blow-up" of the simplex to a cyclohedron, with $n-1$ steps. At each stage k the polytopes that are glued on are a product of a simplex Δ^{n-k} and a cube I^k, where the factors Δ^{n-k} are attached to the codimension k-faces of the original simplex.*

So as not to perturb the flow of the main text, Theorem C and details about the cyclohedron that are not needed in the proof of the Main Theorem are referred to Appendix B.

The organization of the paper is as follows:

We start by giving the combinatorial background and introducing the relevant types of trees in Section 1. Here we also discuss the three operads of Abelian groups with differentials on which the CW models are based. Before introducing said models, we turn to the polytopes that will be used to construct them: simplices, associahedra and cyclohedra in Section 2. Here we give two CW decompositions each of the associahedron and the cyclohedron. The second CW composition is novel and leads to Theorem B. Armed with these results we construct the three relevant CW complexes in Section 3 and prove their relations as expressed in Propositions II–IV; these are Propositions 3.10, 3.14 and 3.15. In the final paragraph of the main text, Section 4, we assemble the results to prove the Main Theorem, Theorem 2.6.

Appendix A gives the relationship to the arc operad and the Sullivan-quasi-PROP, and provides the proofs of Theorem B (Theorem A.5) and Proposition I which, using Definition 3.6, is Proposition 3.11. Finally, in Appendix B, we distill the results on the cyclohedron of the main text to give the sequential blow-up of Theorem C (Theorem B.7) and demonstrate this on the examples of W_3 and W_4.

1. Trees, dg-operads and algebras

1.1. Trees

Let us first recall the standard definitions and then fix the specific technical conditions on the trees with which we will be working.

A *graph* will be a 1-dim CW complex and a *tree* will be a graph whose realization is contractible. We will need some further data. To fix these data, we note that given a graph Γ, the set of 0-cells forms the set of *vertices* $V(\Gamma)$ and the set of 1-cells forms the set of *edges* $E(\Gamma)$. A *flag* is a half-edge. The set of all flags is denoted by $F(\Gamma)$. Notice that there is a fixed point free involution $\iota : F(\Gamma) \mapsto F(\Gamma)$ which maps each half-edge to the other half-edge making up the full edge. Each flag has a unique vertex, which we will call the vertex of the flag. The respective map taking a flag to its vertex will be called ∂. The flags at a vertex v are the half-edges incident to that vertex. The set of these flags will be denoted by $F_v(\Gamma)$. The *valence* of a vertex v is defined to be $val(v) = |F_v(\Gamma)|$.

For us a *ribbon graph* is a graph Γ together with a cyclic order on each of the sets $F_v(\Gamma)$. We impose no condition on the valence of a vertex. The cyclic orders give rise to a map N which assigns to a flag f the flag following $\iota(f)$ in the cyclic order. The iteration of this map gives an action of $\mathbb{Z}$ on the set of flags. The *cycles* are the orbits of this latter map.

An *angle* α of a ribbon graph is a pair of flags $\{f_1, f_2\}$ which share the same vertex $\partial(f_1) = \partial(f_2)$ and where f_2 is the immediate successor of f_1. Notice that these may coincide. The edges of α are $e_i = \{f_i, \iota(f_i)\}$. There is a 1–1 correspondence between flags (or edges) at a vertex and the angles at a vertex.

A ribbon graph is called *planar* if its image can be embedded in the plane in such a way that the induced cyclic orders coming from the orientation of the plane equal the given cyclic orders of the graph.

A globally marked ribbon graph is a ribbon graph with a distinguished flag. A globally marked planar tree is traditionally called *planar planted*. In the tree case, the vertex of the marked flag is called the *root* and denoted by v_{root}; the vertices v with $val(v) = 1$ which are distinct from v_{root} will be called *leaves* and the set of these vertices will be denoted by V_{leaf}.

If a tree is planted, there is a unique orientation towards the root and hence each vertex has incoming edges and at most one outgoing edge, the root being the exception in having only incoming edges. We will sometimes also use the *arity* $|v|$ of v to denote the number of incoming edges to the vertex v. Notice that for all vertices *except the root*, $val(v) = |v| + 1$, but for the root $val(v_{root}) = |v_{root}|$. In the figures, the orientation of the edges toward the root is taken to be downward.

For a tree τ and $e \in E(\tau)$ we will denote the tree τ' obtained from τ by contracting e by $\tau' = \tau/e$. If in a rooted tree the marked flag f_0 is contracted, we fix the new marked flag to be the image of the flag $f_1 = N(f_0)$. In this situation we will also say that τ is obtained from τ' by inserting an edge, and if we want to be more specific we might add "into the vertex v", where v is the image of e under the contraction and write $e \mapsto v$.

If there is a vertex v of valence 2 in a tree, we denote by τ/v the tree τ/e where e is either one of the two edges incident to v. This just removes v and splices together its two edges.

A *black and white (b/w) tree* is a pair (τ, clr), that is a planar planted tree τ whose set of vertices comes equipped with a color map denoted $clr : V(\tau) \to \mathbb{Z}/2\mathbb{Z}$, which satisfies that *all leaves are mapped to* 1 *and the root is mapped to* 0.

We call the inverse images of 0 black vertices and the inverse images of 1 white vertices. The sets of black and white vertices will be denoted by V_{black} and V_{white} respectively. In particular, the condition above then means that *all leaves are white and the root is black*.

In a b/w tree the edges which have two black vertices will be called *black edges* and denoted by E_{black}. Similarly E_{white} denotes the white edges, that is those whose vertices are both white. All other edges will be called *mixed* and denoted by E_{mixed}. When contracting an edge, we fix

that the color of the new vertex is black if the edge was black and white if the edge was white. In the case that the edge is mixed, we fix the color of the new vertex to be white.

A b/w tree is called *bipartite* if all edges are mixed. A b/w tree is called *stable* if there is no black vertex v_b with arity 1, except for the root which is the only black vertex that may have valence (and thus arity) 1, and it may only have valence 1 if its unique incident edge is mixed.

A b/w tree is called *stably bipartite* if the following conditions hold:

(1) There are no white edges.
(2) There are no black vertices of arity 1 and valence 2 with both of its incident edges being black.
(3) There are no black vertices of arity 1 and valence 2 where one edge is black and the other edge is a leaf edge.
(4) The root may have valence 1, but only if its unique incident edge is mixed.

Notice that a stably bipartite tree becomes bipartite when all the black edges are contracted and stable if all the black vertices of valence 2 are removed. Stable trees and stably bipartite trees are closed under contraction of black edges.

The effective white angles of a b/w tree are those angles whose vertices are white *and* which have two distinct flags. They will be denoted by $\angle^w$. All effective white angles of flags at a given white vertex v will be denoted by $\angle^w(v)$.

The conditions above are perhaps not quite obvious from the tree point of view but they are quite natural from an arc/foliation point of view (see Appendix A).

We fix that a b/w subtree of a b/w tree has a white root.

An S-labelled b/w tree is a b/w tree together with a bijective labelling $Lab : S \to V_{white}$; we will write $v_i := Lab^{-1}(i)$. When contracting a white edge, we label the new white vertex by the union of the two labels considered as sets.

We will also need to cut and assemble a tree by gluing subtrees along a tree. The basic operation is *replacing a vertex with a tree*. An example is given in Fig. 1. Combinatorially this is defined as follows. *Replacing a black vertex* v in a planar b/w tree τ by a planar b/w tree τ' whose number of leaves equals $|v|$ and whose root is black means the following: (1) we remove all flags incoming to v from τ; (2) we add all the vertices of τ' that are not leaves and all flags of τ' except the flags incident to the leaves; (3) we "glue in" the new vertices and flags by keeping ι wherever it is still defined and using ϕ and ϕ^{-1} for the other flags, where ϕ is the unique bijection preserving the order of the sets of flags incident to leaves of τ' and the set of incoming flags (observe that ϕ exists since the cardinality of the two sets are the same and both of them have an order). We also fix that the outgoing flag of v has the root of τ' as its vertex.

When *replacing a white vertex* v of a planar b/w tree τ by a planar b/w tree we proceed as follows: (1) we remove the vertex v and all incoming flags of v from τ; (2) we add all the vertices of τ' that are not leaves and all flags of τ' which are not incident to the leaves; and (3) we glue the flags as in the case of replacing a black vertex. There is a special case, in which a white vertex that is adjacent to a root of valence 1 is replaced. In this case, as a final step, we contract the unique edge incident to the root.

See Fig. 1 for an example. The example has extra labellings, which are discussed in Section 3.2.1.

We will deal with three sets of trees in particular:

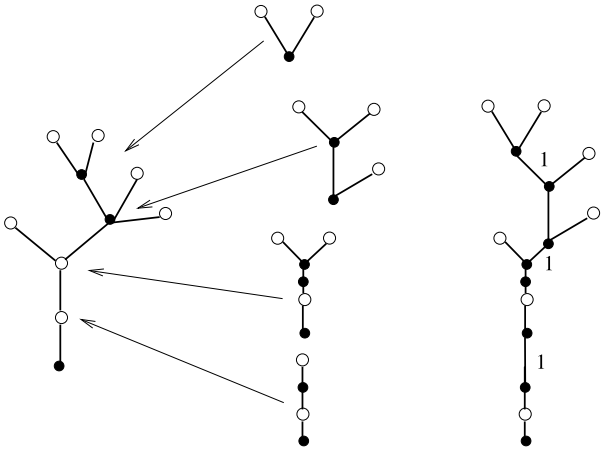

Fig. 1. An example of replacing vertices by trees. In the tree on the left, we replace the vertices with the trees in the middle as indicated to obtain the tree on the right.

Definition 1.1. We define $\mathcal{T}_{bipart}(n)$ to be the set of $\{1,\dots,n\}$-labelled b/w bipartite planar planted trees. We use $\mathcal{T}_{bipart}$ for the collection $\{\mathcal{T}_{bipart}(n), n \in \mathbb{N}\}$.

We recall that we fixed that all leaves of a b/w tree are white and the root is black.

Definition 1.2. We let $\mathcal{T}_{\infty}(n)$ be the set of $\{1,\dots,n\}$-labelled b/w stable planar planted trees. We denote by $\mathcal{T}_{\infty}$ the collection $\{\mathcal{T}_{\infty}(n), n \in \mathbb{N}\}$.

Definition 1.3. We let $\mathcal{T}_{ht}(n)$ be the set of pairs (τ, h), where τ is a black and white $\{1,\dots,n\}$-labelled stably bipartite tree and $h : E_{black}(\tau) \to \{x, 1\}$ is called the height function. The collection $\{\mathcal{T}_{ht}(n), n \in \mathbb{N}\}$ will simply be denoted by $\mathcal{T}_{ht}$.

Here x stands for variable height. We will denote the set of edges labelled with x by E_x.

Notation 1.4. *We will use the notation $\mathbb{Z}S$, for the Abelian group generated by a set S. E.g. $\mathbb{Z}\mathcal{T}_{bipart}(n)$ and $\mathbb{Z}\mathcal{T}_{\infty} = \bigoplus \mathbb{Z}\mathcal{T}_{\infty}(n) = \mathcal{M}$.*

1.2. The differentials

There are natural differentials on each of the three Abelian groups $\mathbb{Z}\mathcal{T}_{bipart}$, $\mathbb{Z}\mathcal{T}_{\infty}$ and $\mathbb{Z}\mathcal{T}_{ht}$. The differential for $\mathcal{T}_{bipart}$ was given in [15] and the one on $\mathbb{Z}\mathcal{T}_{\infty}$ was introduced in [22]. We will briefly recall the definitions and give a new definition for a differential on $\mathbb{Z}\mathcal{T}_{ht}$.

1.2.1. The differential for $\mathbb{Z}\mathcal{T}_{bipart}$

Following [15,14], we fix a tree $\tau \in \mathcal{T}_{bipart}(n)$ for each effective white angle $\alpha \in \angle^w$ and let $\partial(\alpha)(\tau)$ be the tree obtained by *collapsing the angle* α. Combinatorially put, let $\alpha = \{f_1, f_2\}$ and $e_i = \{f_i, \iota(f_i)\}$, and set $v_i = \partial\iota(f_i)$. Then $\partial(\alpha)(\tau)$ is the tree where v_1 and v_2 are identified as are e_1 and e_2. The new marked flag will simply be the image of the original marked flag (see Fig. 2). Using this notation, the differential is defined as

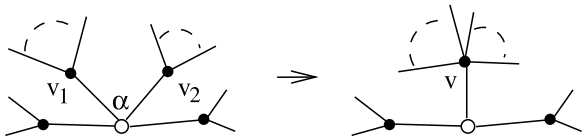

Fig. 2. Collapsing a white angle.

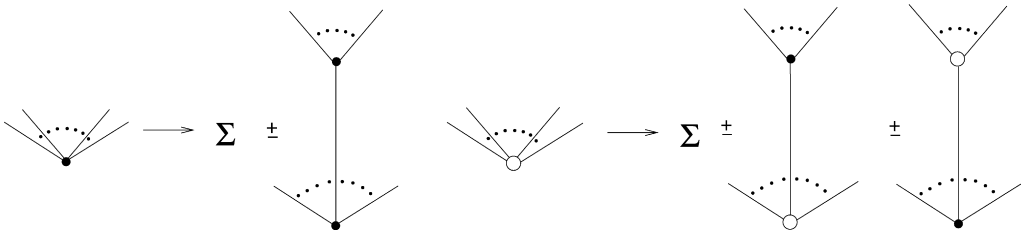

Fig. 3. Differential of $\mathbb{Z}\mathcal{T}_\infty$ on a black vertex and a white vertex. All sums are over stable trees only.

$$\partial(\tau) = \sum_{\alpha \in \angle^w} \pm \partial(\alpha)(\tau) \tag{1.1}$$

1.2.2. The differential on $\mathcal{M} = \mathbb{Z}\mathcal{T}_\infty$

Following [22], we fix a tree $\tau \in \mathcal{T}_\infty(n)$. We will consider all trees that are obtained from τ by adding an edge which is either mixed or black. That is, the summands of the differential are indexed by pairs (τ', e) such that the tree τ'/e obtained by contracting e is equal to τ and $e \in E_{black} \amalg E_{mixed}$. Here the cyclic structure is the induced one and we recall that the rules for contracting edges prescribe that the image of a black edge is a black vertex and the image of a mixed edge is a white vertex:

$$\partial(\tau) = \sum_{\substack{(\tau', e) \\ \tau'/e = \tau,\ e \in E_{black} \amalg E_{mixed}}} \pm \tau' \tag{1.2}$$

Alternatively one can sum over local contributions $\partial(v)(\tau)$ considering only those edges whose image is v. This is the way it is written in [22].

$$\partial(\tau) = \sum_{\substack{v \in V_{white}, (\tau', e) \\ \tau'/e = \tau,\ e \in E_{mixed},\ e \mapsto v}} \pm \tau' + \sum_{\substack{v \in V_{black}, (\tau', e) \\ \tau'/e = \tau,\ e \in E_{black},\ e \mapsto v}} \pm \tau' \tag{1.3}$$

A sketch of the trees involved in the sums is given in Fig. 3.

1.2.3. The differential on $\mathbb{Z}\mathcal{T}_{ht}$

We now fix $(\tau, h) \in \mathcal{T}_{ht}(n)$. For the differential, we will sum

(a) over collapsing the white angles, i.e. elements of $\angle^w$ (see Fig. 2) and
(b) over contracting or re-labelling the black edges labelled by x (see Fig. 4).

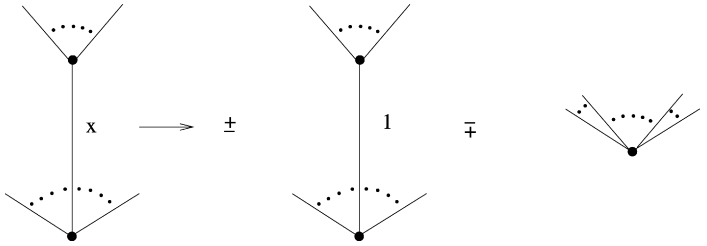

Fig. 4. Differential of $\mathbb{Z}\mathcal{T}_{ht}$ on an edge in E_x.

For a white angle $\alpha \in \angle^w$, we again let $\partial_\alpha(\tau)$ be the tree with the white angle collapsed. We can keep the height function since collapsing the angles does not affect the set of black edges—only two mixed edges are identified. For an edge $e \in E_x \subset E_{black}$ we set $\partial_e(\tau, h) = (\tau, h') - (\tau/e, h|_{E_{black}\setminus e})$ where $h'(e) = 1$ and $h'(e') = h(e')$ for $e \neq e'$. The differential is now

$$\partial(\tau) = \sum_{\alpha\in\angle^w} \pm\partial_\alpha(\tau) + \sum_{e\in E_x} \pm\partial_e(\tau) \tag{1.4}$$

1.2.4. Signs

As usual the fixing of sign conventions is bothersome, but necessary. The quickest way is to use tensor products of lines of various degrees indexed by the sets of edges and/or angles. See [14,15,22] for detailed discussions. Here line refers to a free object on one generator shifted to the appropriate degree, e.g. $\mathbb{Z}[-1]$ or $k[1]$. One way to fix an order of the tensor factors is to fix an enumeration of all flags by going around the planar planted tree starting at the marked flag and then using the map ι and the cyclic order to enumerate. Hence all vertices, the subset of white vertices, angles, the subset of white angles, and edges are enumerated by counting them when their first flag appears. We will call this the *planar order*. To fix the signs one simply fixes weights of the elements of the ordered sets.

A third way, and perhaps the cleanest for the present discussion, is to use the geometric boundary of polytopes as we will discuss in Section 3 below. In particular, the signs for the different types of trees are fixed by Eqs. (3.1), (3.2) and (3.4).

Proposition 1.5. *In all three cases $\mathcal{T}_{bipart}, \mathcal{T}_\infty, \mathcal{T}_{ht}$, the map ∂ satisfies $\partial^2 = 0$.*

Proof. In all cases this is a straightforward calculation. The signs are such that inserting two edges or alternatively collapsing two edges or angles (or one edge and one angle) in different orders yields the same tree, but with opposite signs, since these elements are ordered and formally of odd degree in any of the above formalisms. □

1.2.5. The maps π_∞ and i_∞

There are maps $\pi_\infty : \mathbb{Z}\mathcal{T}_\infty \to \mathbb{Z}\mathcal{T}_{bipart}$ and $i_\infty : \mathbb{Z}\mathcal{T}_{bipart} \to \mathbb{Z}\mathcal{T}_\infty$ which were defined in [15].

The first map π_∞ is given as follows: if there is a black vertex of valence > 3, then the image is set to be 0. If all black vertices are of valence 3, we (1) contract all black edges and (2) insert a black vertex into each white edge, to make the tree bipartite. It is clear that the leaves will stay white. The global marking, viz. root is defined to be the image of the marking under the contraction.

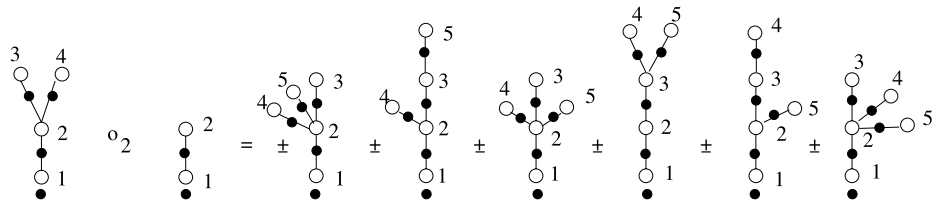

Fig. 5. Composition of two trees in $\mathcal{T}_{bipart}$. The subtrees on the right corresponding to the inserted tree have white vertices labelled by 2 and 3.

The second map i_∞ is given as follows: (1) Remove all black vertices whose valence equals 2 and (2) replace each black vertex of valence > 2 by the binary tree, with all branches to the left. This is of course not symmetric, but any choice will do. We now see that π_∞ is surjective, since $\pi_\infty \circ i_\infty = \mathrm{id}$.

Lemma 1.6. *(See [15].) The map π_∞ behaves well with respect to the differential. $\pi_\infty(\partial(\tau)) = \partial\pi_\infty(\tau)$.*

Proof. This is a straightforward calculation; see [15]. □

1.3. Operad structures on $\mathbb{Z}\mathcal{T}_{bipart}$ and $\mathcal{M} = \mathbb{Z}\mathcal{T}_\infty$

Both the operad structures are what one could call an insertion operad structure. They have been previously defined in [15] and in [22] respectively. The latter was defined combinatorially in [22], but also can be induced from the topological level; see Appendix A and Proposition 3.11.

There are two equivalent ways to describe this type of operation. The indexing is always over the white vertices. Inserting a tree τ' into a tree τ at the vertex v_i means the signed sum over all trees τ'' which contain τ' as a subtree such that $\tau''/\tau' = \tau$ with the image of τ' being v_i:

$$\tau \circ_i \tau' = \sum_{\tau'':\, \tau''/\tau'=\tau,\, \tau' \mapsto v_i} \pm\tau'' \tag{1.5}$$

Here one also fixes that τ'' be either in $\mathcal{T}_{bipart}$ or $\mathcal{T}_\infty$, and τ' is treated as a labelled subtree whose labels are given by shifting by $i-1$.

Also, there is a small technical point when contracting τ' as a subtree in the case of $\mathcal{T}_{bipart}$. In the contraction of such a subtree, we do not contract the root edge of the subtree. The result would not be bipartite otherwise as there would be two neighboring white vertices. Alternatively, we can insert an additional black edge for the black root of the subtree, such that the new vertex has valence 1 when considered as a vertex of the subtree, and then contract the full subtree.

In the case of a stable tree, there is the provision that if the root of τ' has valence 1 then as above, the root edge is contracted before identifying τ' as a subtree, i.e. this vertex is not present in the subtree. The sign again is given by one of the schemes in Section 1.2.4.

Alternatively, one can describe a 3-step procedure consisting of first cutting off all the branches over v_i, then grafting τ' into v_i, and finally grafting the branches back to τ' keeping their order as induced by the cyclic order on τ. We refer to [22,13–15] for more details. An example of the operation for bipartite trees is given in Fig. 5.

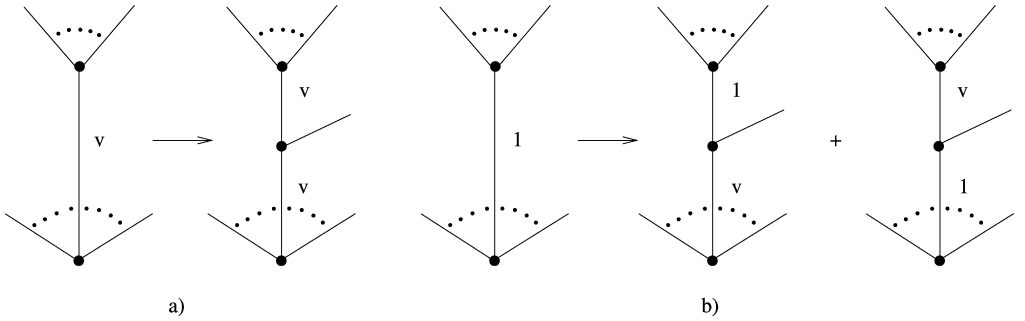

Fig. 6. Gluing a branch into an edge a) in E_x and b) of height 1.

Proposition 1.7. *(See [22,15].) The collections $\mathcal{T}_\infty$ and $\mathcal{T}_{bipart}$ are dg-operads.*

Proposition 1.8. *(See [15, Proposition 1.5.8].) π_∞ is a morphism of dg-operads.*

1.3.1. Operad structure on $\mathbb{Z}\mathcal{T}_{ht}$

Strictly speaking, we will not need an operad structure on $\mathbb{Z}\mathcal{T}_{ht}$ to prove the Main Theorem. However, there is indeed an operad structure, and it and the operad structure on $\mathbb{Z}\mathcal{T}_{bipart}$ can be understood as special cases of an operad structure induced by the quasi-PROP structure of Sullivan chord diagrams of [16]; see Appendix A.

We first give the definition combinatorially. Given (τ, h) and (τ', h') we define $\mathcal{S}$ to be the following set of trees with height (τ'', h''): τ'' is obtained by cutting the branches of τ above v_i, gluing in τ' at v_i and then gluing in the branches in their planar order to the white angles of the image of τ' and into the black edges $E_{black}(\tau')$. To glue a branch into an edge, we add a vertex to the edge and glue the branch to this new vertex. The admissible height functions h'' coincide with the original height functions on all images of edges of $E_{black}(\tau)$ and all unaffected edges of $E_{black}(\tau')$. Let e be a black edge that has been split into n black edges by gluing in $n-1$ branches. If $e \in E_x$ then *all* the values of h'' on the edges it is split into are x. If e is labelled by 1, then all but one of the labels are x and one label is 1. All of these labels are allowed; see Fig. 6

$$(\tau, h) \circ_i (\tau', h') = \sum_{(\tau'', h'') \in \mathcal{S}} \pm(\tau'', h'') \tag{1.6}$$

Proposition 1.9. *The collection $\mathbb{Z}\mathcal{T}_{ht}$ yields a dg-operad.*

Proof. Somewhat tedious but straightforward calculation; or see Proposition A.4. □

1.3.2. A_∞ algebras

Notice that the trees $\mathcal{T}_{pp}$ in $\mathcal{T}_\infty$ with $V_{white} = V_{leaf}$ form a sub-operad $\mathbb{Z}\mathcal{T}_{pp}$ of $\mathbb{Z}\mathcal{T}_\infty$.

It is straightforward to see that this operad is isomorphic to the operad of planar planted trees with labelled leaves with the operation of grafting at the leaves. Keeping this in mind the following definition goes back to Stasheff (see [26] for a more complete history):

Definition 1.10. An A_∞ algebra is an algebra over the dg-sub-operad $\mathcal{T}_{pp}$.

In particular, on an A_∞ algebra A there is an n-ary operation μ_n for each $n \in \mathbb{N}$, such that μ_1 is a differential ∂, and μ_2 is associative up to the homotopy $\partial(\mu(3))$. After this there is a whole tower of homotopies governed by the combinatorial structure of the K_n.

1.3.3. Associative algebras

We can also consider $\mathbb{Z}\mathcal{T}_{cor}$, that is the bipartite trees with white leaves only, as a sub-operad of $\mathbb{Z}\mathcal{T}_{bipart}$.

Lemma 1.11. *$\mathbb{Z}\mathcal{T}_{cor}$ is isomorphic to the operad for associative algebras.*

2. Polytopes and trees

In this section, we review associahedra and cyclohedra emphasizing that they together with the standard simplex can be thought of as compactifications of the open simplex. This in turn has an interpretation as a configuration space.

2.1. Simplices

We let Δ^n be the standard n-simplex and $\dot{\Delta}^n$ be its interior.

2.1.1. Configuration space interpretation

If we realize the simplex as $\Delta^n = \{t_1, \dots, t_n \mid 0 \leqslant t_1 \leqslant \cdots \leqslant t_n \leqslant 1\}$ and $\dot{\Delta}^n = \{t_1, \dots, t_n \mid 0 < t_1 < \cdots < t_n < 1\}$, then $\dot{\Delta}^n$ is the configuration space of $n+1$ distinct points on $\dot{I} = (0,1)$ and the closure just allows the points to collide with each other or with 0 and 1. That is, the space is just the compactification obtained from n unlabelled, not necessarily distinct, points on $[0,1]$.

The interior of this compactification is the same as considering n distinct points on S^1 with one point fixed at 0. The compactification then distinguishes if the points collide from the right or left with 0, but keeps no other information.

2.1.2. Tree interpretation

As a polytope, the simplex is a CW complex and of course the cells are again just simplices. We can give a tree interpretation as follows: the cell defined by an n-simplex will be indexed by a tree $*_n^w$ which we call a white star. The tree $*_n^w$ is the unique bipartite tree with exactly one white vertex that is not a leaf, of which there are n, and all of whose non-root black vertices have valence 2 and whose root has valence 1. We can pictorially think of the white vertex as S^1 and the incident edges as indicating the points on S^1, where the root marks 0. The boundary map is just the sum of the collapsing of the white angles. After collapsing angles, we still have only one white non-leaf vertex, but the non-root black vertices may acquire valence $\geqslant 3$ or the root may have valence $\geqslant 2$. The leaves incident to a black non-root vertex are the points that have collided with each other and the leaves incident to the root are the points that collided with 0. Since the tree is planar, we can distinguish if this happened from the right or left.

2.1.3. Topological interpretation

We can make the cell decomposition above topological as follows. To each white angle of $*_n^w$ we associate a number in $(0,1]$, that is we have a map $w : \angle^w(*_n^w) \to (0,1]$, which we subject to the condition that the total angle at the white vertex is 1: $\sum_{\alpha \in \angle^w} w(\alpha) = 1$. If the only white angle is not effective, we can just label it by 1. We can imagine that these angles measure the

distance between the points of S^1 in units of 2π. The open part is then just $\dot{\Delta}^n$ and the closure is Δ^n. The boundary comes from sending the length of the angles to zero and collapsing the angles.

2.2. Associahedra

The associahedra are abstract polytopes introduced by Stasheff [29,30] and fittingly are also called Stasheff polytopes. The vertices of the associahedron K_n correspond to the possible full (i.e. lacking ambiguity) bracketings of the expression $(a_1 \cdots a_n)$, e.g. $(((a_1a_2)a_3)(a_4a_5))$. Each such bracketing can be depicted as a planar planted tree by thinking of the bracketing as giving rise to a flow chart. The dimension l faces correspond to bracketings which are missing l pairs of brackets; here it is assumed that the outside bracketing is fixed and always present. The highest dimension and hence the dimension of K_n is $n-2$. We will also allow and use $K_2 = pt$. As an example the face corresponding to $((a_1a_2)a_3a_4)$ is of dimension 1 and $(a_1a_2a_3a_4)$ is of dimension 2. The boundary of the faces is given by inserting one set of brackets in all possible ways. In the tree picture the codimension is given by the number of internal, that is non-leaf edges and the boundary map is defined by inserting an edge in all possible ways. It is a well-known fact that the faces of K_n are products $K_i \times K_{n-i+1}$.

2.2.1. Labelling

It will be convenient to use other indexing sets and consider S-labelled associahedra K_S where S is an arbitrary finite set. In the bracket formalism this is the indexing set of the elements a_i. This is already useful in the description of the boundary, since the boundary components are distinguished by different labels. In particular the boundary is given by

$$\partial K_n = \sum_{(I',I''):\ |I'|\geqslant 2,\, |I''|\geqslant 2} K_{I'} \times K_{I''} \tag{2.1}$$

where $I' = \{j, \ldots, j+k\}$ with $1 \leqslant j, k \geqslant 1$, $j+k \leqslant n$ and $I'' = \{1, \ldots, j-1, I', j+k+1, \ldots, n\}$. This choice corresponds to the bracketings compatible with $(a_1 \cdots a_{j-1}(a_j \cdots a_{j+k}) \times a_{j+k+1} \cdots a_n)$. Notice that $|I''| = n - |I'| + 1$. All the indices in I' are contracted to a single index in I''.

2.2.2. Configuration interpretation

The space K_n can be viewed as a "real Fulton–MacPherson compactification" [1,7] of the space of $n-2$ distinct points on the interval $(0,1)$ [26]. The information kept is the relative speeds of multiple collisions. Just as above, by identifying 0 and 1 one can view this as a compactification of distinct points on S^1, where now one keeps track separately of the points colliding with 0 from the right and from the left and of the relative speeds of these two processes.

2.2.3. A first CW realization with stable trees $\mathcal{T}_{pp}$

As an abstract polytope the associahedra are naturally CW complexes. The cells for K_n are indexed by planar planted trees with n leaves and their dimension is given by $n-2-|E|$. We will make the leaves white and consider them to live in $\mathcal{T}_\infty(n)$ and insist that the labelling from 1

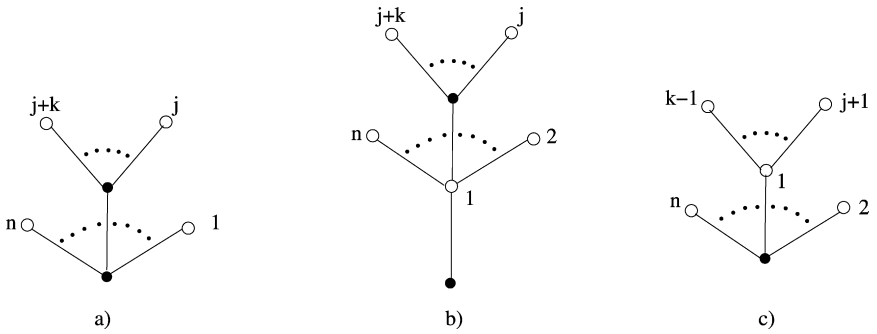

Fig. 7. a) Boundary trees of K_n, b), c) boundary trees of W_n.

to n be consistent with their planar order. To be precise we let $\mathcal{T}_{pp}(n)$ be the trees in $\mathcal{T}_{\infty}(n)$ whose only white vertices are leaves. Each cell $C(\tau)$ represented by a tree $\tau \in \mathcal{T}_{pp}(n)$ is a product

$$C(\tau) = \bigtimes_{v \in V(\tau)} K_{|v|} \tag{2.2}$$

The differential given by taking the boundary agrees with the sum over all possibilities of inserting a black edge which is the one inherited from $\mathcal{T}_{\infty}$, i.e. $\partial(C(\tau)) = C(\partial(\tau))$, where we extend C in the obvious fashion to linear combinations. Notice that the labelling sets are now induced by contracting either all the edges of the "upper" vertex or alternatively contracting all the edges of the "lower" vertex; see Fig. 7 a).

2.2.4. A second CW realization with trees with heights $\mathcal{T}_{pp}^{ht}$

There is an alternative natural CW structure which is actually a cubical decomposition of the associahedra. This is sometimes called the Boardman–Vogt decomposition [3]. Strictly speaking it is a Boardman–Vogt construction for the operad of monoids which happens to give a decomposition for the associahedra; see also [26,22]. The cells of this compactification are cubes and are indexed by particular trees in $\mathcal{T}_{ht}$. The trees are those in which all the white vertices are leaves, viz. $\mathcal{T}_{pp}(n)$ and we again insist that their planar order be defined by the labelling. Putting all possible height functions on them, we obtain a subset $\mathcal{T}_{pp}^{ht}(n) \subset \mathcal{T}_{ht}(n)$. The cell indexed by τ is

$$C(\tau) = I^{E_x} = \bigtimes_{e \in E_x} I \tag{2.3}$$

The boundary is given by using the differential of $\mathcal{T}_{ht}$. We again have that $\partial(C(\tau)) = C(\partial(\tau))$, where we extend C in the obvious fashion to linear combinations.

Remark 2.1. Notice that this CW decomposition is a subdivision of the first. The cells of the finer decompositions that belong to a given cell given by a tree τ can be described as follows: first label all black edges of τ by 1 and then consider all trees in $\mathcal{T}_{ht}$ which can be contracted to τ and whose labels match on the non-contracted edges.

Remark 2.2. We actually rediscovered this decomposition from the arc point of view; see Appendix A. After presenting the results, we realized that this decomposition coincides with a

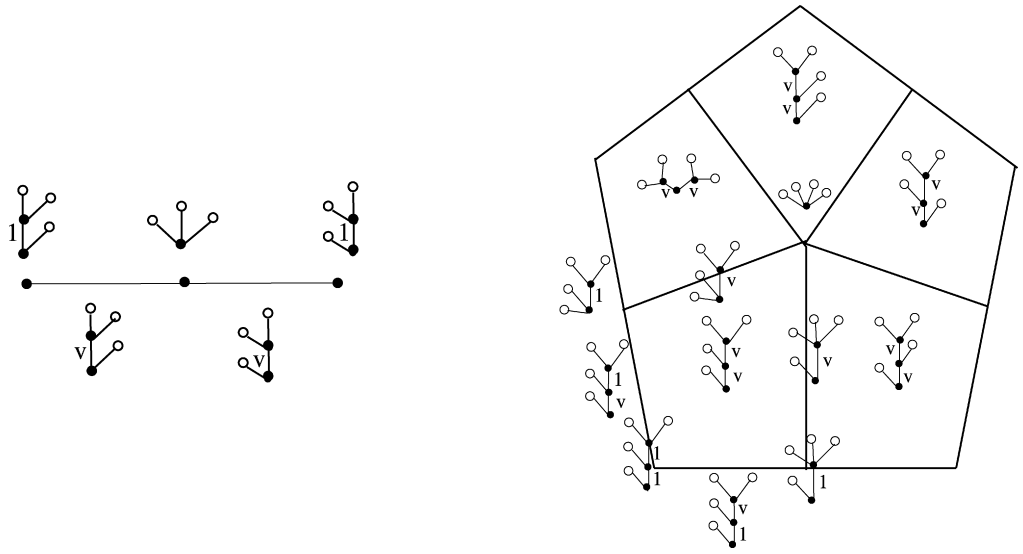

Fig. 8. The decompositions of K_3 and K_4. For K_4 the trees of dimension less than 2 are only given for the lower-left cell.

Boardman–Vogt construction, but we would like to point out that it also comes naturally from a topological quasi-operad; see Appendix A.

2.2.5. A topological realization via trees with heights

Since their introduction, people have looked for convex polytope realizations of the associahedra. The first such resolution was given in [11], see also [28]. This has led to several nice results and constructions; see e.g. [5,6,8,23] for recent results and also [26] for more references and details.

Taking the cue from the above cell decomposition one can easily give a natural realization which is *not a convex polytope*, but a *PL* realization. For this we will consider the trees with bounded heights, that is pairs (τ, w) where $\tau \in \mathcal{T}_{pp}^{ht}$ and $w : E_{black} \to (0, 1]$. If we let $\mathcal{E}(n)$ be the set of all possible black edges for such trees with fixed n, this space is naturally a *subspace* on $\mathbb{R}^{\mathcal{E}(n)}$.

Notice that in the subspace topology the limit where $h(e) \to 0$ for some edge e is naturally identified with the tree with heights, where this edge has been contracted. Moreover the boundaries are also naturally given by the same PL realization.

Proposition 2.3. *The construction above yields a PL realization of K_n.*

Notice that these realizations are not convex polytopes. Rather they are "broken" into convex subpieces. As an example K_3 of Fig. 8 is the union of the two intervals $I = [0, 1]$ and $I'[0, 1]$ along 0 which is realized inside $\mathbb{R}^2$ as $I = [0, 1] \times \{0\}$ and $I' = \{0\} \times [0, 1]$. In fact, there are realizations in terms of convex polytopes as we remarked above and abstractly, our realizations give subdivisions of these as convex polytopes. In our setup of trees with heights they are however already realized naturally by the coordinates describing the heights of "all possible edges".

Definition 2.4. We call a topological height function w on a tree with heights (τ, h) *compatible* if $w(e) = 1$ when $h(e) = 1$ and $w(e) \in (0, 1)$ when $h(e) = x$.

The elements inside a given cell (τ, h) are then the elements (τ, w) with $\tau \in \mathcal{T}_{pp}$ and w a compatible topological height function. The elements in the closure of this set, that is those on the boundary of the cell are those pairs (τ', w) where τ' can be obtained from τ by contracting any number of edges of E_x, w may now take values in $(0, 1]$, and at least one edge is contracted or one edge $e \in E_x$ has $w(e) = 1$.

2.3. Cyclohedra

The cyclohedra are abstract polytopes introduced by Bott and Taubes [4]. The vertices of the cyclohedron W_n correspond to the possible full cyclic bracketings of the expression $a_1 \cdots a_n$, e.g. $a_1))(a_2(a_3$. The l-dimensional sides are given by the bracketings missing l brackets. Here we allow the empty bracketing. The boundary map is given by inserting one pair of brackets in all possible ways. The dimension of W_n is $n-1$. We will also allow and use $W_1 = pt$. Moreover, as with the K_n, we will need to consider S-labelled W_n, that is W_S, where S is the indexing set of the elements.

It is well known and easy to check that in this formalism, the $codim(l)$ cells are products of l polytopes of which at most one is a cyclohedron, and the others are associahedra. The possible sub-bracketings of a cyclic bracketing are given by independent choices of regular bracketings.

From the description above, we see that the boundary is given by

$$\partial(W_n) = \sum_{(I', I'')} W_{I'} \times K_{I''} \tag{2.4}$$

Here the indexing sets on the right-hand side are the ordered sets $I'' = (j, j+1, \ldots, j+k)$ $j \leqslant 1$, $j + k \leqslant n$ for $k \geqslant 1$ and $I' = (1, \ldots, j-1, I'', j+k+1, \ldots, n)$, or $I'' = (2, \ldots j, \{1, j+1, \ldots, k-1\}, k, k+1, \ldots, n)$ for $j < k$ and $I' = (\{1\} \cup I'', j+1, \ldots, k-1)$. If $k+1 = j$, this means that $I' = (1)$.

Again these indexing sets follow from contracting the relevant edges of the "upper" or "lower" vertex; see Fig. 7 b), c).

2.3.1. A configuration interpretation

The way they were originally introduced by Bott and Taubes they are the blow-up of a configuration space. This is also related to the Axelrod–Singer [1] compactification of configuration space; see [26] for details. In particular, the cyclohedron W_n is the compactification of the configuration of n distinct points on S^1 with one point fixed at 0; see [26] for details.

2.3.2. A first CW realization in terms of stable trees $\mathcal{T}_{cyclo}$

Again, we have the natural structure of a CW complex. A tree depiction is given as follows: we consider trees which are $\{1, \ldots, n\}$-labelled b/w stably bipartite with at most one white internal vertex labelled by 1 and all other white vertices being leaves which are labelled commensurate with the planar order. This means that if there is an internal white vertex, all the leaves are labelled $2, \ldots, n$ in that order and if there is no internal white vertex, all white vertices are leaves and the order of the leaves labelled $2, \ldots, n$ is exactly this order, while the vertex labelled by 1 may appear anywhere in the planar order. We will call these trees $\mathcal{T}_{cyclo}$. The "big" cell representing

the whole cyclohedron is the unique tree which has no black vertices. Again, we can think of the internal white vertex as S^1 and its edges as indicating the location of the points, if we wish.

The boundary comes from inserting a mixed edge into the white non-leaf vertex, which yields a product of a cyclohedron and an associahedron.

In general we have that the cell of τ is given by

$$C(\tau) = \bigtimes_{v\in V_{white}} W_{val(v)} \times \bigtimes_{v\in V_{black}} K_{|v|} \tag{2.5}$$

The differential is then the differential of $\mathcal{T}_\infty$, $\partial(C(\tau)) = C(\partial(\tau))$, where we extend C in the obvious fashion to linear combinations.

2.3.3. A second CW realization in terms of trees with heights

We will exhibit another CW realization for W_n which has the following trees as an indexing set: the set of trees $\mathcal{T}^{ht}_{cyclo}$ in $\mathcal{T}_{ht}$ which have n white vertices and at most one white non-leaf vertex. We consider these trees to be labelled by $\{1,\dots,n\}$ and impose the same conditions as for $\mathcal{T}_{cyclo}$, i.e. the vertices $v_2,\dots,v_n$ are leaves and the planar order of this subset is the one written. The vertex v_1 may be internal and may appear anywhere in the planar order of all white vertices, even if it is a leaf.

We define a cell of such a tree as

$$C(\tau) = \bigtimes_{v\in V_{white}} \Delta^{|v|} \times I^{E_x} \tag{2.6}$$

We now get a CW complex $K^{cyc}(n)$ by using the trees above and the differential of $\mathcal{T}_{ht}$ to define the boundary and hence the attaching maps.

To fix terminology we will call a black vertex *potentially unstable* if it is adjacent to a non-leaf mixed edge.

Lemma 2.5. *The following statements hold for the CW complex $K^{cyc}(n)$:*

(i) *The dimension of $|K^{cyc}(n)|$ is $n-1$. The top-dimensional cells are precisely indexed by the trees such that there are only $n-1$ leaves, the arity of all black vertices is $\leqslant 2$, all potentially unstable non-root vertices are valence* 2*, the root is either not potentially unstable or if it is, it is of arity* 1*,* and *all black edges are labelled by x.*

(ii) *All* 0*-cells are indexed by trees whose white vertices are all leaves, and all black edges have height h equal to one.*

(iii) *All k-cells are in the boundary of $k+1$ cells for $k < n-1$ and each chain of cells such that the successor is in the boundary of the predecessor has length n.*

(iv) *The codimension* 1 *cells are given by trees of the following types:*
   (a) *A tree as in* (i) *with only one black edge labelled by* 1.
   (b) *A tree as in* (i) *but with one of the non-root potentially unstable vertices having valence* 3.
   (c) *A tree as in* (i) *but with one of the other black vertices (not potentially unstable) of valence* 4.
   (d) *A tree as in* (i) *but the root vertex not potentially unstable having valence* 3.
   (e) *A tree as in* (i) *but the root vertex potentially unstable and of valence* 2.
   (f) *A tree as in* (i) *but no internal white vertex.*

Each cell of the types (b), (c), (d) *and* (e) *are in the boundary of precisely* 2 *top-dimensional cells and the cells of type* (a) *and* (f) *are in the boundary of exactly one top-dimensional cell.*

Proof. For statement (i), by counting dimensions, we see that the dimension of cells listed is indeed $n-1$. It is also just a dimension count that these cells are indeed the maximal ones. Any higher arity of a black vertex or a black edge labelled by anything else but x will lead to a dimension drop as one could change the label to x, insert a new edge, or "split" an angle.

This procedure also shows the claims (ii) and (iii). The chains are given by a series of a total number of $n-1$ contractions and collapsing.

To be in codimension 1 the dimension count has to go down by 1 from the top-dimensional cells by moving to the boundary. Starting with a top-dimensional cell indexed by a tree with heights, we can (1) re-label an edge from x to 1, (2) contract an edge labelled by x or (3) collapse one white angle. The result of (1) will be a tree of type (a), the result of (2) will be of type (b) if the edge was incident to a potentially unstable vertex and of type (c) if it was not and not incident to the root. It will be of type (d) if it was adjacent to the root and after contraction the root is not potentially unstable. It is of type (e) if the root becomes potentially unstable.

The results of (3) will be of type (b) if the angle did not have the root as one of its vertices and will be of type (e) or (f) if it did. This may only occur if the root had valence 1.

To determine the cells that lead to the particular boundary, we reverse the above operations in all possible ways. In case (a) we can only re-label the edge by x and in case (f) the only possibility is to "split" the angle of the vertex labelled by 1 at the root in order to obtain a non-leaf white vertex.

In case (b) the only two possibilities are to insert a black edge labelled x or to "split" the vertex into a white angle. In case (c) there are exactly two different ways to insert one black edge labelled by x, which is analogous to the case of K_3. Case (d) is also analogous. Finally, in case (e) we can either insert an edge marked x to make the root not potentially unstable, or split the angle. □

Theorem 2.6. *The CW complex $K^{cyc}(n)$ is a CW realization of the cyclohedron. This is a refinement of the polytope CW complex. The additional* 0*-cells correspond to the refinement of the associahedra.*

Proof. We will make the argument by induction. We have to show that the boundary of $K^{cyc}(n)$ is indeed composed of $W_{n-i} \times K_i$'s with $i \geqslant 2$. First the cases of $n = 1, 2$ are trivial to check. Here we use a decomposition of these polytopes viewed as cell complexes known by induction for the cyclohedra and the previous results for the associahedra. The case $n = 3$ is in Fig. 9, and the case of $n = 4$ is worked out in Appendix B. We let $\omega(n) = \sum_{\tau:\ \dim(C(\tau))=n-1} \tau$ be the sum of all top-dimensional cells. Now $\partial\omega = \sum \partial\tau$ and on the right-hand side we will only have the terms of types (a) and (f) of the lemma above, since the terms of type (b)–(e) cancel out. For terms of type (f) we notice that they sum to associahedra K_n, labelled by the different orders of $1, \ldots, n$ which respect the natural order of $2, \ldots, n$, i.e. all the faces of the cyclohedron which are associahedra, using the second CW decomposition described above. For terms of type (a) we first notice that the cells are products of the cells associated to the trees above and below the black edge marked by one. To be precise, given a tree τ of the type (a) with the edge e marked by 1 we let τ' be the tree with e and all the edges above e contracted and τ'' be the subtree of τ above e. Then the cell $C(\tau) = C(\tau') \times C(\tau'')$. The cell $C(\tau'')$ has no internal white vertex and

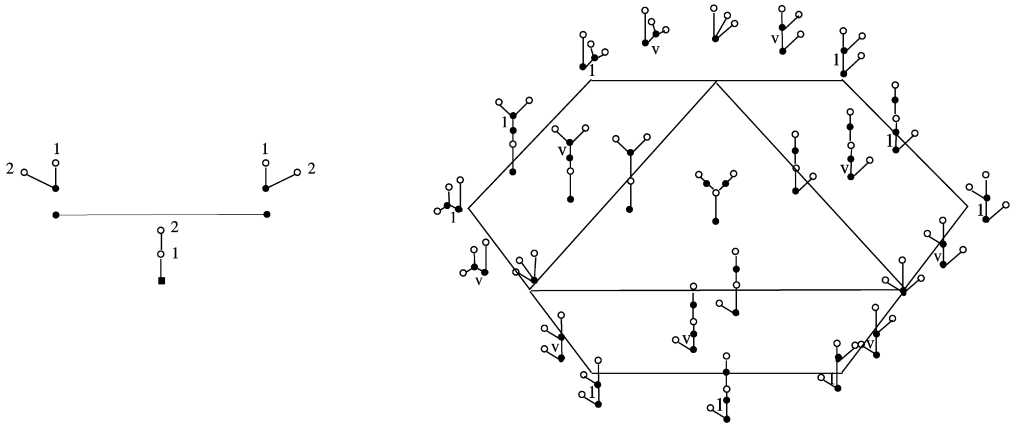

Fig. 9. The decomposition of W_2 and W_3. The labels for the white vertices of W_3 are omitted. As depicted, the special vertex labelled 1 is always the lowest white vertex on the center "stem" of the tree.

is part of an associahedron. The cell $C(\tau)$ has a white vertex and by induction this is part of a lower dimensional W_k. Fixing either tree, i.e. τ' or τ'', and regarding all the possible trees they can come from, we see that the summands needed to complete the associahedron (as discussed in Section 2.2.4) and the cyclohedron (as in the assumption) are all realized per induction for the boundary terms of lower dimension. Moreover, it is straightforward to check that all the needed labellings enumerated in Eq. (2.4) are realized and are only those. By Lemma 2.5 the CW complex composed of the consolidated cells (i.e. the unions of smaller cells) then yields an abstract polytope and this polytope is the cyclohedron W_n.

Finally, the 0-cells are indexed by trees with no effective white angles, and hence all white vertices are leaves. All the black edges are labelled by 1 and hence correspond exactly to the 0-cells of the respective associahedra. □

2.3.4. A topological realization

Let $Cyc^{top}(n)$ be the set of pairs (τ, w) where $\tau \in \mathcal{T}_{cyclo}$ is one of the trees above with n white vertices and $w : E(\tau) \to \mathbb{R}_{>0}$ which satisfy:

(1) For all $e \in E_{black}$, $w(e) \leqslant 1$.
(2) For all $\alpha \in \angle^w$: $\sum_{\alpha \in \angle^w(v)} w(e) = 1$.

For convenience, we extend w to all angles at white vertices by marking those that only have one flag by 1. This set obtains a topology induced by collapsing angles and contracting edges whose w goes to zero. It is clear that this realizes the cell complex and hence:

Proposition 2.7. *Cyc^{top} is a topological PL realization of W_n for the new CW decomposition and the original CW decomposition.*

2.4. Contracting the associahedra and cyclohedra

There is a flow on the two realizations which contracts all black edges; for $0 \leqslant t < 1$: $\Psi(t)((\tau, w)) = (\tau, \psi(t)(w))$ where

$$\big(\psi(t)(w)\big)(\alpha) = w(\alpha) \quad \text{for } \alpha \in \angle^w$$
$$\big(\psi(t)(w)\big)(e) = (1-t)w(e) \quad \text{for } e \in E_x,\ 0 \leqslant t < 1$$

and $\Psi(1)(\tau, w) = (\tilde{\tau}, w|_{\tilde{\tau}})$ where $\tilde{\tau}$ is the tree τ with all black edges contracted and $\tilde{w}$ is w restricted to $\tilde{\tau}$, that is restricted to the white angles, which remain "unchanged" during the construction. Here "unchanged" means that the sets are in natural bijection and we use this bijection to identify them.

Lemma 2.8. *The flow contracts $Cyc^{top}(n)$ to Δ^n and K_n to a point and establishes homotopy equivalences, in fact strong deformation retracts, between these pairs of spaces.*

Proof. Using the previous descriptions of the polytopes involved, it is clear that Ψ gives a flow whose image is the purported one. □

3. Three CW models, K^1, K^∞ and K^{ht}, for the little discs and their relations

3.1. Three CW models

The basic idea is to form products of the polytopes of the last section to obtain CW complexes from the various types of trees $\mathcal{T}_{bipart}, \mathcal{T}_\infty, \mathcal{T}_{ht}$. For $\mathcal{T}_{bipart}$ this has been done in [15], which is what we first recall.

3.1.1. The model K^1 a.k.a. $\mathcal{C}act^1$

Definition 3.1. (See [15].) We define the CW complex $K^1(n)$ to be the following CW complex: the k-cells are indexed by $\tau \in \mathcal{T}_{bipart}(n)$ with $\sum_{v \in V_{white}(\tau)} |v| = k$, where the cell corresponding to a tree is defined to be

$$C(\tau) := \bigtimes_{v \in V_{white}} \Delta^{|v|} \tag{3.1}$$

The attaching maps are given by using the differential ∂ on $\mathcal{T}_{bipart}$: $\partial(C(\tau)) = C(\partial(\tau))$ where we use the orientation and signs dictated by the ordering in Eq. (3.1).

Remark 3.2. This complex was called $\mathcal{C}act^1(n)$ in [14,15].

The elements in this CW complex are pairs (τ, w) where $\tau \in \mathcal{T}_{bipart}$ and w is a topological "height" or "weight" function as in Section 2.1.3; that is a function $w : \angle^w \to (0, 1]$ such that $\forall v \in V_{white}$: $\sum_{\alpha \in \angle^w(v)} w(\alpha) = 1$. Note that there are no black edges. The main theorem concerning this complex is:

Theorem 3.3. *(See [14,15].) $|K^1|$ is a quasi-operad which induces an operad structure on $CC_*(K^1)$ which in turn is a chain model for the little discs.*

We recall that a topological quasi-operad or quasi-PROP only has to be associative up to homotopy (see [14] for the definition of quasi-operad and [16] for the definition of quasi-PROP). We do not require any higher compatibility on the topological level, since we are ultimately only interested in the chain level. As it turns out, and this a main part of the "magic" of our

constructions, all our structures are already strict on the chain level. Furthermore, even more is true for the quasi-operads in which we are interested, namely, there are even rectifications to strict topological operads.

3.1.2. The model K^∞, a CW realization of $\mathcal{M}$

Definition 3.4. (See [15].) We define the CW complex $K^\infty(n)$ to be the following CW complex. The k-cells are indexed by $\tau \in \mathcal{T}_\infty(n)$ with $\sum_{v\in V_{white}(\tau)} |v| + \sum_{v\in V_{black}} (|v|-1) = k$. The cell corresponding to a tree is defined to be

$$C(\tau) := \bigtimes_{v\in V_{white}} W_{val(v)} \times \bigtimes_{v\in V_{black}} K_{|v|} \tag{3.2}$$

The attaching maps are given by using the differential ∂ on $\mathcal{T}_\infty$: $\partial(C(\tau)) = C(\partial(\tau))$ where we use the orientation and signs dictated by the ordering in Eq. (3.2).

Lemma 3.5. *The complexes $\mathcal{M}(n)$ and $CC_*(K^\infty(n))$ are isomorphic over $\mathbb{Z}$.*

Proof. By construction the two Abelian groups are isomorphic. Their dg-structures are also compatible by the combinatorics of the previous section and the construction. Explicitly, the boundary of the cell is given by

$$\begin{aligned}\partial\big(\Delta(\tau)\big) = &\sum_{v\in V_{white}} \pm \partial W_{val(v)} \times \bigtimes_{v'\in V_{white}\setminus\{v\}} W_{val(v')} \times \bigtimes_{v''\in V_{black}} K_{|v''|} \\ &+ \sum_{v\in V_{black}} \pm \bigtimes_{v'\in V_{white}} W_{val(v')} \times \partial K_{|v|} \times \bigtimes_{v''\in V_{black}\setminus\{v\}} K_{|v''|}\end{aligned} \tag{3.3}$$

where now each summand corresponds to inserting an edge which is mixed for the first sum and black for the second sum. This shows that $\mathcal{M}(n)$ and $CC_*(K^\infty)(n)$ are isomorphic complexes. □

Definition 3.6. The *induced operad structure* on $CC_*(K^\infty) := \{CC_*(K^\infty(n))\}$ is the one induced by the isomorphisms $CC_*(K^\infty) \cong \mathcal{M}$.

3.1.3. A new mediating model K^{ht}

Definition 3.7. (See [15].) We define the CW complex $K^{ht}(n)$ to be as follows. The k-cells are indexed by $(\tau, h) \in \mathcal{T}_{ht}(n)$ with $\sum_{v\in V_{white}(\tau)} |v| + |E_x| = k$. The cell corresponding to a tree is defined to be

$$C(\tau) := \bigtimes_{v\in V_{white}} \Delta^{|v|} \times I^{E_x} \tag{3.4}$$

The attaching maps are given by using the differential ∂ on $\mathcal{T}_{ht}$: $\partial(C(\tau)) = C(\partial(\tau))$ where we use the orientation and signs dictated by the ordering in Eq. (3.4).

Lemma 3.8. *Each element of $|K^{ht}(n)|$ corresponds to a pair (τ, w) with τ a $\{1,\dots,n\}$-labelled stably bipartite tree and "heights/weights" given by $w : E_{black}(\tau) \cup \angle^w \to (0,1]$ with the condition that $\sum_{\alpha\in\angle^w(v_w)} w(\alpha) = 1$ for all $v_w \in V_{white}$.*

We will call the set of all these pairs $\mathcal{T}_{ht}^{top}$.

Proof. Any element p of $|K^{ht}|$ lies inside a unique maximal cell. This corresponds to a tree $\tau \in \mathcal{T}_{ht}$. For a black edge $e \in E_x(\tau)$, we can thus define $w(e)$ to be the coordinate of p in the factor I^e in $C(\tau)$; for the black edges of τ of height $h(\tau) = 1$ we set $w(e) = 1$, and for $\alpha \in \angle^w(v)$, $w(\alpha)$ will be given by the barycentric coordinates on $\Delta^{|v|} \subset \mathbb{R}^{val(v)}$. □

3.1.4. Quasi-operad structure on $|K^{ht}|$

Just as for $|K^1|$ above, we can define a quasi-operad structure on the topological level, that is on $|K^{ht}|$, which induces an operad structure on the chain level. We achieve this via an arc interpretation to realize the space basically as a sub-quasi-PROP of the Sullivan-quasi-PROP [16].

Proposition 3.9. *$|K^{ht}|$ is a topological quasi-operad and the quasi-operad maps are cellular and induce an operad structure on $CC_*(K^{ht}) \simeq \mathbb{Z}\mathcal{T}_{ht}$.*

Proof. See Appendix A, Proposition A.4. □

3.2. The relations between the three complexes

3.2.1. K^{ht} is a refinement of K^{∞}

Proposition 3.10. *K^{ht} is a refinement of K^{∞}, i.e. they have the same realization, and each cell of K^{ht} is contained in a unique cell of K^{∞}.*

Proof. To show that $|K^{\infty}| \simeq |K^{ht}|$ we notice that each point $p \in |K^{\infty}|$ lies in a unique maximal cell indexed by a stable tree $\tau \in \mathcal{T}_{\infty}$. Each cyclohedron $W_{val(v)}$ or associahedron $K_{|v|}$ appearing as a factor indexed by a vertex v of $C(\tau)$ has a decomposition as in Section 2 and our element p lies inside a unique one of these finer cells. These finer cells are of the type $\Delta^k \times I^l$ and are indexed by a tree with heights $\tilde{\tau}(v) \in \mathcal{T}_{ht}$, for each vertex v. The coordinates in these cells uniquely determine the projection to the appropriate factor of $C(\tau)$ corresponding to the factor $W_{val(v)}$ or $K_{|v|}$. To obtain a pair $(\tilde{\tau}, w) \in \mathcal{T}_{ht}^{top}$ as in Lemma 3.8, we proceed as follows: for each non-leaf v insert the tree $\tilde{\tau}(v)$ into the vertex v, the result of which is a stably bipartite tree $\tilde{\tau}$. We define the function w to be given by the coordinates of p w.r.t. the $C(\tilde{\tau}(v))$ for the white angles and the new black edges and the markings 1 for the black edges stemming from the original tree.

Vice versa, given a point $p \in |K^{ht}|$, that is a pair (τ, w), we claim that we can identify it with a point in one of the finer cells in the decomposition of K^{∞} above. The cell of K^{∞} in which this point lies will be indexed by the tree obtained by contracting all non-leaf, non-root edges of τ which are not labelled by 1 and forgetting the function w. Each pre-image of a vertex, after adding white leaves, will be of the type $\mathcal{T}_{pp}^{ht}$ or $\mathcal{T}_{cyclo}^{ht}$ with a compatible topological height function w. By the previous paragraph this uniquely determines a point in $|K^{\infty}|$.

It is easy to see that these maps are homeomorphisms that are inverses of each other. It then follows from the definition of the maps that each cell of K^{ht} is contained in a unique cell of K^{∞}. □

For an example of the above procedure see Fig. 1.

Using this proposition, the operad structure on $CC_*(K^\infty)$ which was introduced via the *ad hoc* Definition 3.6 above can now be induced for the topological level. In other words, it can be replaced for Proposition I, which in its precise form reads:

Proposition 3.11. *The operad structure of $CC_*(K^{ht}) \simeq \mathbb{Z}\mathcal{T}_{ht}$ pulls back to $\mathcal{M} \simeq \mathbb{Z}\mathcal{T}_\infty \simeq CC_*(K^\infty)$ and this operad structure coincides with the induced operad structure of Definition* 3.6.

Proof. See Appendix A. □

3.2.2. $|K^{ht}|$ contracts to $|K^1|$

Using basically the same flow as in Section 2.4 but now extended to all of $|K^{ht}|$, that is pairs (τ, w), we can give an explicit deformation retraction.

Definition 3.12. We define the flow $\Psi : I \times |K^{ht}| \to |K^{ht}|$ by $0 \leqslant t < 1$: $\Psi(t)((\tau, w)) = (\tau, \psi(t)(w))$ where

$$\psi(t)(w)(\alpha) = w(\alpha) \quad \text{for } \alpha \in \angle^w$$
$$\psi(t)(w)(e) = (1-t)w(e) \quad \text{for } e \in E_x,\ 0 \leqslant t < 1$$

and $\Psi(1)(\tau, w) = (\tilde{\tau}, w|_{\tilde{\tau}})$ where $\tilde{\tau}$ is the tree τ with all black edges contracted and $\tilde{w}$ is w restricted to $\tilde{\tau}$, that is restricted to the white angles, which remain "unchanged" during the construction. Here "unchanged" again means that the sets are in natural bijection and we use this bijection to identify them.

Definition 3.13. We define $\iota : |K^1(n)| \to |K^{ht}(n)|$ by mapping a pair (τ, w) giving a point in $|K^1|$ to itself, but now considered as specifying a point in $|K^{ht}|$.

This is possible, since a bipartite tree τ is stably bipartite and since a bipartite tree has no black edges and hence $E_{black}(\tau) \cup \angle^w(\tau) = \angle^w(\tau)$.

Proposition 3.14. *The topological spaces $|K^{ht}(n)|$ and $|K^1(n)| = \mathcal{C}act^1(n)$ are homotopy equivalent and the homotopy is given by the explicit flow Ψ. This in fact yields a strong deformation retract $r(n)$ of $|K^{ht}(n)|$ onto the image of $\iota(|K^1|(n))$ and a cellular map.*

Proof. It is clear that Ψ is a homotopy and easy to see that it contracts onto the image of ι, which remains fixed under the homotopy. This yields the desired statement. □

Proposition 3.15. *The sequence of maps $\pi_\infty^{top}(n) : |K^\infty(n)| \xrightarrow{\sim} |K^{ht}(n)| \xrightarrow{r(n)} |K^1(n)|$ induces a quasi-isomorphism of operads $\pi_\infty : \mathcal{M} \simeq CC_*(K^\infty) \to CC_*(K^1)$ on the chain level.*

Proof. First by Propositions 3.10 and 3.14 the composition is cellular and hence indeed induces a map on the cellular chain level. We see that any cell of $\mathcal{T}_\infty$ is contracted to a cell of lower dimension as soon as there is a black vertex whose valence is greater than 3, so that these cells are sent to zero. This corresponds to the fact that Ψ contracts all the associahedra to a point. If the vertices only have valence 3 then the black subtrees are contracted onto the image of ι which

yields a cell of the same dimension indexed by the tree $\pi_\infty(\tau)$. Finally, we know by Lemma 1.6 that π_∞ is an operadic map. Since π_∞^{top} is a homeomorphism followed by a strong retraction, the map induced in homology is an isomorphism. □

Theorem 3.16. *K^∞ is a cell model for the little discs operad whose cells are indexed by $\mathcal{T}_\infty$.*

Proof. By Theorem 3.3, $K^1 = CC_*(Cact^1)$ is an operadic chain model for the little discs, hence by the last proposition we may deduce that K^∞ also has this property. □

4. The A_∞ Deligne conjecture

In this section, we give the solution to the above conjecture using our results combined with the action of the minimal operad $\mathcal{M}$ of [22]. We first review this operation briefly. Recall that given a tree in $\mathcal{T}_\infty(n)$ there is a natural action on the Hochschild complex by viewing the tree as a flow chart. In particular, given functions $f_1, \dots, f_n$, the action of $\tau \in \mathcal{T}_\infty(n)$ is defined as follows: first "insert" each of the functions f_i into the corresponding white vertex v_i and then view the tree as a flow chart using the operations μ_l of the A_∞ algebra at each black vertex of arity l and the brace operation $f_j\{g_1, \dots, g_k\}$ at each white vertex of arity k to concatenate the functions, where f_j is the function associated to the vertex v and the g_i are the functions which are obtained by following the k flow charts above v corresponding to the k different branches.

The brace operations are defined as [10,12,33]

$$h\{g_1, \dots, g_n\}(x_1, \dots, x_N) := \sum_{\substack{1 \leqslant i_1 \leqslant \dots \leqslant i_n \leqslant |h|: \\ i_j + |g_j| \leqslant i_{j+1}}} \pm h\big(x_1, \dots, x_{i_1 - 1}, g_1(x_{i_1}, \dots, x_{i_1 + |g_1|}), \dots, x_{i_n - 1}, g_n(x_{i_n}, \dots, x_{i_n + |g_n|}), \dots, x_N\big) \tag{4.1}$$

Theorem 4.1 *(Main Theorem). There is a cell model K^∞ for the little discs operad, whose operad of cellular chains $CC_*(K^\infty)$ acts on the Hochschild cochains of an A_∞ algebra inducing the standard operations of its homology on the cohomology. Moreover, this is minimal in the sense that the cells correspond exactly to the natural operations obtained by concatenating the functions and using the A_∞ structure maps.*

Proof. This follows from Theorem 3.16 in conjunction with the theorem of [22] that the operad $\mathcal{M} \simeq \mathcal{T}_\infty$ acts in a dg-fashion on Hochschild cochains of an A_∞ algebra. □

Acknowledgments

It is a pleasure to thank J. Stasheff, S. Devadoss and J. McClure for interesting and useful discussions. R.K. would also like to thank the Max-Planck-Institute for Mathematics in Bonn, Germany, for its kind hospitality and support.

Appendix A. Connection to arcs and polygons with diagonals

In this appendix, we give the connection of the CW complexes to the arc operad of [20] and the Sullivan-quasi-PROP of [16]. All of the (quasi-) operad structures with which we are concerned are based on the two mentioned structures, and we use these facts to give proofs of Theorem B

and Proposition I. There are actually three different pictorial realizations for the same objects: arc graphs, ribbon graphs and trees. These correspondences have been worked out in full detail in [15,16,18], and we will content ourselves with a brief review of the salient features referring the fastidious reader to these papers.

A.1. The arc picture

First we would like to recall that an element of $\mathcal{DA}rc$ is a surface $F^r_{g,n+1}$ of genus g with $n+1$ boundary components labelled by $\{0,\dots,n\}$ and r punctures with marked boundary, that is one marked point per boundary component together with two sets of data, an arc graph and weights.

An arc graph is a collection of arcs, that is embedded curves, from boundary to boundary that

(1) do not hit the marked points;
(2) do not intersect;
(3) are not parallel. This means that they are not homotopic to each other, where the endpoints may not cross endpoints of other arcs or the marked points;
(4) are not parallel to a part of the boundary, where now the marked points are included into the boundary;
(5) as a set, provide each boundary with at least one incident arc

considered up to the action of the pure mapping class group that keeps all punctures and marked points pointwise fixed and the boundaries setwise fixed.

Weights for an arc graph are given by assigning a weight to each arc, that is a map from the set of all arcs to $\mathbb{R}_{>0}$. We will only need to consider $g = r = 0$ in the present discussion and we *fix this from now on*.

A.1.1. Gluing in the arc picture

The gluing is understood as a gluing of partially measured foliations, which can be paraphrased as follows: we realize the arcs with weights as bands with width, and if two sets of bands incident to two boundaries have the same total width, we simply splice them together along their leaves. That is, glue the bands and cut along the common partition.

The different operad/quasi-operad/quasi-PROP structures [20,16] are basically built in the same fashion. First pick two boundaries to be glued, then scale such that the weights agree, and finally glue the boundaries and the foliations as explained above. We will have a new feature for $|K^{ht}|$ since the topological gluing will involve a forth step of renormalizing.

Regardless of this there are two parts to the gluing, one combinatorial, where the combinatorics govern the types of arcs that occur, and the second topological, which is the part dictated by the particular weights. On the chain level, we only want to keep the combinatorics.

A.2. Embedding $|K^{ht}|$ into $\mathcal{DA}rc$ and generalized cacti

Just as there is a topological embedding of $\mathcal{C}act^1$ into the arc operad $\mathcal{A}rc$ of [20], there is also such an embedding of $|K^{ht}|$ into $\mathcal{A}rc$. We let $\mathcal{L}in\mathcal{T}ree_\infty$ be the subspace which consists of those arc families that are of genus 0 with no punctures, arcs running only from the boundary marked by i to the boundary marked by 0 *and possibly* arcs running from 0 to 0, which satisfy the following conditions: there is a representative of projective weights on the arcs such that

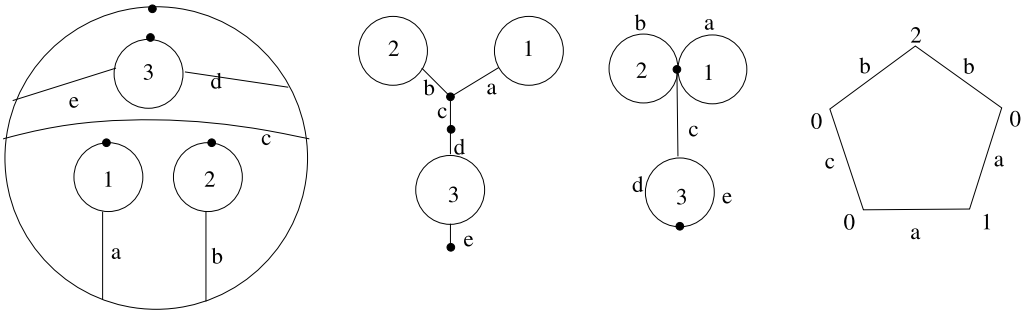

Fig. 10. An arc graph, its tree, cactus representation and *one* of its polygons.

(1) no arc running from 0 to 0 homotopic to a boundary i together with one arc from i to 0 where the marked point is considered to be part of the boundary;
(2) the linear orders at the boundaries i are (anti)-compatible with the linear order at 0. That is, if for two arcs a and b which hit the boundary i $a <_0 b$ in the order at 0, then we have $a >_i b$ in the order at the boundary i.

The space $|K^{ht}|$ corresponds to the subset $\mathcal{L}in\mathcal{T}ree^1_\infty \subset \mathcal{L}in\mathcal{T}ree_\infty$, which additionally satisfies that

(3) the weight of each arc from 0 to 0 is $\leqslant 1$;
(4) the sum of the weights for each boundary except 0 is 1.

In the following, we give a brief translation primer for the different combinatorial pictures. An example is given in Fig. 10.

A.2.1. From arc graphs to ribbon graphs

Given an arc family in $\mathcal{A}rc$ we first define its dual ribbon graph. This has one vertex for each complementary region and one edge for between the two (not necessarily distinct) regions on the different sides of each arc. See [14,15] for more details. Every cycle of the ribbon graph corresponds to exactly one boundary component. Since the boundary components were oriented and marked, the ribbon graph will be marked as well, that is, there is one distinguished flag in each cycle that points in the direction of the orientation and has its vertex in the region that contains the marked point.

Notice that in our case, since all arcs run to zero, there is a distinguished cycle which runs through all the edges. That is, the ribbon graph is tree-like in the terminology of [16]. In this correspondence each arc corresponds to an edge, and hence if the arcs have weights, so have the edges.

A.2.2. From ribbon graphs to trees

For a tree-like ribbon graph, define its *incidence graph* to be given by one white vertex for each cycle excluding the distinguished one and a black vertex for each previous vertex, where we join two black vertices if they are joined in the original graph along an edge which does not belong to the non-distinguished cycles and we join a white and a black vertex if the black vertex lies on the cycle given by the white vertex. The tree is rooted and planted by taking the

flag corresponding to the marked flag of the graph as the marked flag of the tree. Now the edges correspond to the white angles and black edges and hence these carry the weights.

A.2.3. From $\mathcal{T}_{ht}$ trees to ribbon graphs

Given a tree in $\mathcal{T}_{ht}$ we first "blow-up" the white vertices to cycles and then contract all the images of the mixed edges. In the blowing up process each angle becomes an edge of the ribbon graph with the two flags of the angle incident to the two vertices of the new edge preserving their orders. The labels are now on all of the edges.

A.2.4. From ribbon graphs to arc graphs

It is well known that thickening a ribbon graph gives rise to a surface with an embedding of the ribbon graph as the spine. Taking the dual graph on the surface basically yields an arc graph. For the missing markings, we mark the respective boundary of the respective region containing the marked flag of the cycle. The weights pass along the bijection of the edges and the markings. We refer to [15] for more details.

A.2.5. Description of $\mathcal{T}_{ht}$ in terms of polygons

By the above procedure every tree in $\mathcal{T}_{ht}$ translates to an element in $\mathcal{DA}rc$. Cutting along the arcs decomposes the surface into pieces, and, as we fixed that $g = s = 0$ above, these pieces are polygons. These polygons are $2n$-gons with sides alternatingly corresponding to pieces of the boundary and arcs. We obtain a set of polygons by contracting all sides corresponding to boundaries and call these the complementary polygons.

We have the following translation table

$\mathcal{T}_{ht}$	$\mathcal{DA}rc$
Mixed edge	Arc from 0 to $i \neq 0$
Black edge	Arc from 0 to 0
There are no white edges	The tree is an intersection graph
There are no black vertices of valence 2 both of whose edges are black	No parallel arcs
There are no black vertices of valence 2 with one edge black and the other edge a leaf edge *unless* the vertex is the root	There are no triangles among the complementary polygons, where two edges correspond to the same arc
Trees obtained by cutting black edges are marked by 1	Complementary regions of the arcs from 0 to 0 are of weight 1

A.2.6. Generalized spineless cacti

Yet another way to picture the trees is to look at the ribbon graph as a new version of cacti. Here one is now allowed to have edges between the lobes. We define $\mathcal{C}act_\infty$ to be the space of metric marked ribbon graphs corresponding to the subspace $\mathcal{L}in\mathcal{T}ree_\infty$ of $\mathcal{DA}rc$.

Proposition A.2. *$\mathcal{L}in\mathcal{T}ree_\infty$ is a sub-operad and hence $\mathcal{C}act_\infty$ is an operad.*

Proof. The claim boils down to checking that the conditions of $\mathcal{LinTree}_\infty$ are stable under gluing, which they are. □

We also let $\mathcal{Cact}^1_\infty$ be the space of ribbon graphs corresponding to $\mathcal{LinTree}^1_\infty$.

A.2.7. Gluing in $\mathcal{Cact}_\infty$

The gluing operation defined above is reminiscent of the definition of the gluing of $\mathcal{Cact}$ as defined in [14]. If we are given two generalized normalized spineless cacti $c_1, c_2 \in \mathcal{Cact}^1_\infty$ then $c_1 \circ_i c_2$ is the generalized normalized spineless cactus obtained as follows: glue c_2 into the cycle marked by i of c_1 by identifying the cycle 0 of c_2 with the cycle marked by i of c_1, where these cycles are considered to be parameterized over S^1 by the metric on their edges and their marked points. Here it is important that we scale the total length, i.e., the sum of weights of all the edges of τ' to fit the sum of the weights of the edges of the lobe i of τ. For the quasi-PROP structure, we will scale the other way around, that is scale the lobe to fit. Also to fit the combinatorics, we will need to renormalize this construction.

A.3. The Sullivan-quasi-PROP of [16]

We briefly review the Sullivan-quasi-PROP of [16], but refer the reader to [16] for details.

In order to make contact with the quasi-PROP structure, we need to additionally assume that the boundary labels of the surfaces in question are divided into *In* and *Out* boundaries with labels. Correspondingly we will obtain spaces $\mathcal{DArc}(In, Out)$. If $|In| = n$ and $|Out| = m$ this is naturally a collection of $\mathbb{S}_n \times \mathbb{S}_m$ modules. We will simplify and fix $In = \{1, \ldots, n\}$, $Out = \{1, \ldots, m\}$.

We let $\mathcal{DSul}$ be the collection of subspaces of the spaces of $\mathcal{DArc}(In, Out)$ in which there are only arcs running from the *In* to the *Out* and possibly from the *Out* to the *Out* boundaries *and* there is no empty *In* boundary. This space was denoted $\overline{\mathcal{DArc}^{i \leftrightarrow i}}$ in [16]. We define $\mathcal{DSul}^1 \subset \mathcal{DSul}$ to be the subspace of graphs whose sum of weights of arcs incident to every *In* boundary vertex is 1 and whose arcs from *Out* to *Out* have weights $\leqslant 1$. This is naturally a CW complex.

In [16] we defined the quasi-PROP compositions on $\mathcal{DSul}$ by scaling the input marked by i individually to the weight of the output marked by j it is glued to. This yields topological quasi-PROP structure $\bullet_{i,j}$. Notice that in the gluings one only scales at the *In* boundaries which are to be glued so that the weights on the *In* boundaries which remain after gluing are unchanged as are the weights of the arcs from *Out* to *Out* boundaries. Hence $\mathcal{DSul}^1$ is a sub-quasi-PROP.

Proposition A.3. *The compositions $\bullet$ define a quasi-PROP structure on the cell complex $\mathcal{DSul}^1$.*

Proof. First, the fact that $\mathcal{DSul}^1$ is a cell complex follows in the previous pattern. The cells are just indexed by the relevant graphs. It is clear that $\mathcal{DSul}^1$ is stable under composition. □

Although the PROP structure $\mathcal{DSul}^1$ is cellular, it does not directly yield exactly the dg-PROP structure we are looking for. To make the proofs simpler we again restrict to $g = s = 0$ and deal only with the special sub-structure in which we are interested. Namely, we consider $\mathcal{LinTree}_\infty(n)$ as a subspace of $\mathcal{DSul}^1(n, 1)$ if we declare 0 to be in *Out* and all other inputs to be in *In*. We will identify $\mathcal{Cact}_\infty$ with $\mathcal{Cact}_\infty$ and we will also use the term *lobe* for a cycle corresponding to an *In* boundary.

We will also call an arc black if it runs from 0 to 0 as it will give rise to a black edge and we will call the other arcs white arcs, as they will give rise to white angles.

A.3.1. Renormalized gluing in $\mathcal{L}in\mathcal{T}ree^1_\infty$

In the gluing procedure of the quasi-PROP given by $\bullet$, black bands might be split and although this will induce the right kind of combinatorics on the topological level, it actually yields the wrong type of combinatorics on the chain level. This is simply due to the fact that after splitting a band it can never have weight 1. In order to rectify the situation, we define a slightly modified gluing procedure $\bar{\bullet}$ as follows. First glue according to $\bullet$ and then for each black arc that is split into n arcs we re-scale according to the radial projection $\Delta^{n-1} \to I^n$ that maps the simplex homeomorphically to the faces of I^n which have one or more entries equal to 1. To be precise, if the black arc that is split has weight w and the n arcs it splits into have weights $t_1, \dots, t_n$ with $\sum t_i = W$, then we re-scale the weights to $(\tilde{t}_1, \dots, \tilde{t}_n)$, which is the image of $(t_1, \dots, t_n)$ under the radial projection onto the cube $[0, W]^n$.

Proposition A.4. *$\mathcal{L}in\mathcal{T}ree^1_\infty$ is a sub-CW complex of $\mathcal{D}Sul^1$ and hence a CW complex. The operations $\bar{\bullet}$ endow $\mathcal{L}in\mathcal{T}ree^1_\infty$ with a topological quasi-operad structure, which is equivalent as a quasi-operad to its topological sub-quasi-PROP structure.*

Furthermore, the operations $\bar{\bullet}$ induce an operad structure on $CC_*(\mathcal{L}in\mathcal{T}ree^1_\infty)$ and moreover $CC_*(\mathcal{L}in\mathcal{T}ree_\infty) \simeq \mathbb{Z}\mathcal{T}_{ht}$. The same statements hold true for $\mathcal{C}act^1_\infty$, by identifying it with $\mathcal{L}in\mathcal{T}ree^1_\infty$.

Proof. It is clear that $\mathcal{L}in\mathcal{T}ree^1_\infty$ is a sub-CW complex and stable under the quasi-PROP compositions. The difference between $\bullet$ and $\bar{\bullet}$ is the radial projection which is homotopic to the identity and hence the two structures are both associative up to homotopy and this homotopy gives the equivalence.

Now by taking the intersection graph of a ribbon graph, we see that additively $CC_*(\mathcal{L}in\mathcal{T}ree^1_\infty) = CC_*(\mathcal{C}act^1_\infty) = \mathbb{Z}\mathcal{T}_{ht}$. Taking the composition $\bar{\bullet}$ means that indeed we are allowed all the combinations of putting branches into the angles and into the black edges. The former corresponds to the splitting of a white arc and the latter to the splitting of a black arc. Now $\bar{\bullet}$ was chosen so that inserting into a black edge gives exactly the summands corresponding to the distribution of labels. It is straightforward to check that these gluings are now strictly associative. □

A.3.2. Sub-quasi-PROP structure of $|K^\infty|$ and $|K^{ht}|$

Theorem A.5 *(Theorem B). The realizations $|K^\infty| \simeq |K^{ht}|$ and $|K^1|$ are all topological quasi-operads and sub-quasi-PROPs of the Sullivan-PROP $\mathcal{D}Sul^1$. There is also a renormalized quasi-operad structure such that the induced quasi-operad structures on their cellular chains $CC_*(K^\infty) \simeq \mathbb{Z}\mathcal{T}_\infty$, $CC_*(K^{ht}) \simeq \mathbb{Z}\mathcal{T}_{ht}$ and $CC_*(K^1) \simeq \mathbb{Z}\mathcal{T}_{bipart}$ are operad structures and coincide with the respective combinatorial operad structure on the trees. Moreover, all these operad structures are models for the little discs operad.*

Proof of Theorem A.5 and Proposition 3.11. Taking the intersection graph of the elements of $\mathcal{C}act^1_\infty$ we obtain precisely $|K^{ht}|$ so that the claims for K^{ht} follow from Propositions A.3 and A.4. Now by the cellular map that identifies $|K^\infty|$ with K^{ht}, each cell of K^∞ is a sum of cells of K^{ht}. What we must show is that composing sums of these cells indeed gives a sum of cells. This is most easily demonstrated using $\mathcal{C}act^1_\infty$. In this language the argument is analogous to the one in [15]. Explicitly we claim that if c_1 and c_2 are elements of fixed cells $C(\tau_1)$ and $C(\tau_2)$ of K^∞, that is a sum of cells of K^{ht}, as they vary throughout these cells $c_1 \circ_i c_2$ produces exactly the elements of the cells corresponding to the tree $\tau_1 \circ_i \tau_2$. This is obvious if one considers c_2 as a

subgraph of $c_1 \circ_i c_2$ whose white vertices are re-labelled according to the operad composition. This then allows us to extract c_1 and c_2 from the data and $c_1 \circ_i c_2$ uniquely after we fix the number of lobes of c_1 and c_2 and include these and the label i into the data as well. Hence looking at a possible configuration in $C(\tau_1 \circ_i \tau_2)$ we see that it comes precisely from one c_1 and c_2 via $\circ_i$. This proves the claims about the chain level of K^∞ in Theorem A.5 and Proposition 3.11.

On homology all these models induce the same structure. The map π_∞ is operadic and the same is true for the one induced by the retraction. On homology the operad structure is known by [14] to be isomorphic to the homology of the little discs operad. □

We can actually also prove a little more:

Theorem A.6. *$|K^\infty| \simeq |K^{ht}|$ are equivalent as topological quasi-operads to the sub-operad $\mathcal{L}in\mathcal{T}ree_\infty$ which in turn is equivalent to the little discs operad.*

Proof. It is clear that $\mathcal{L}in\mathcal{T}ree_\infty$ is a sub-operad of $\mathcal{DA}rc$. For both $\mathcal{L}in\mathcal{T}ree_\infty$ and $\mathcal{L}in\mathcal{T}ree^1_\infty$, we can simultaneously scale to length 0 all the edges running from 0 to 0. This gives a homotopy equivalence of $\mathcal{L}in\mathcal{T}ree_\infty$ with the model $\mathcal{C}act$ for the little discs operad (see [14]) and of $\mathcal{L}in\mathcal{T}ree^1_\infty$ with the equivalent model $\mathcal{C}act^1$. Furthermore, if for $\mathcal{L}in\mathcal{T}ree_\infty$ we also scale the weights on the other edges at the same time so that they sum up to 1 on each boundary, we can directly contract it to $\mathcal{C}act^1$. Another way to see the homotopy equivalence of $\mathcal{L}in\mathcal{T}ree_\infty$ and $\mathcal{L}in\mathcal{T}ree^1_\infty$ is to notice that the sum of the weights on the boundaries $1, \ldots, n$ contributes a contractible factor of $\mathbb{R}^n_{>0}$. Hence we have homotopy equivalences of both spaces with $\mathcal{C}act^1$ and it is a straightforward check that this is through homotopies of quasi-operads. This can be done analogously to the argument for $\mathcal{C}act^1$ relative to $\mathcal{C}act$ given in [14]. Hence both are equivalent to $\mathcal{C}act^1$ and thus to each other and the little discs operad (as quasi-operads). □

Appendix B. Sequential blow-ups/downs for the cyclohedron

The subdivision of the cyclohedron by the trees with heights $\mathcal{T}^{ht}_{cyclo}$ gives us an explicit way to blow up the simplex. For this we notice that the number of black edges marked by x gives a depth function $depth(\tau) = |E_x|$. In the top-dimensional cells of W_n $depth(\tau) + val(v) = n$. Here v is the special vertex labelled by 1 that is allowed to be a non-leaf vertex.

Theorem B.7 *(Theorem C). There is a new decomposition of the cyclohedron W_{n+1} into a simplex and cubes. Correspondingly, there is an iterated "blow-up" of the simplex to a cyclohedron, with $n-1$ steps. At each stage the objects that are glued on are a product of a simplex Δ^{n-k} and a cube I^k where the factors Δ^{n-k} are attached to the codimension k-faces of the original simplex.*

Proof. We use the depth function to index the iteration. There is only one element of depth 0 and this corresponds to the simplex. This is step 0 and the starting point of the iteration. All trees of higher depth have a product of a simplex and a cube as their cell. Furthermore, we notice that for a new edge in E_x to appear in a tree indexing an adjacent maximal cell, we first have to collapse one effective white angle. Hence we obtain an iteration for the gluing of the maximal cells, by first collapsing one angle, then allowing to collapse two angles and so on. This iteration according to the number of angles collapsed is precisely by depth. Finally, the Δ^{n-k} factors are

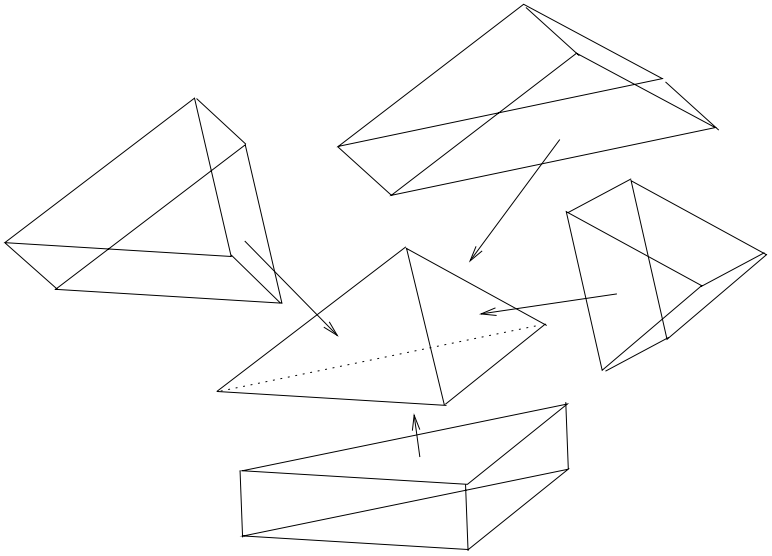

Fig. 11. Step 1: gluing on four $\Delta^2 \times I$s to Δ^3.

naturally identified with the codimension k faces of Δ^n as they correspond to collapsing k angles, and the choices for these angles are precisely indexed by the different faces; see Section 2.1. □

In the first step one "fattens" the faces of the simplex Δ^n by gluing a $\Delta^{n-1} \times I$ onto each face and in the last step one simply glues in cubes.

We illustrate this for W_3 and W_4. The figure for W_3 is Fig. 9, where there is only one blow-up.

Depth 0. This is the simplex Δ^2.
Depth 1. The new elements are products $\Delta^1 \times I = I^2$. There are exactly 3 of these which are glued onto the sides of Δ^2.

This gives a nonegon, but by identifying 3 pairs of sequential sides and all the top-dimensional cells, we are left with the usual hexagon picture; see Fig. 9.

For W_4 there are two blow-ups and the details are illustrated in Fig. 15.

Depth 0. This is the simplex Δ^3.
Depth 1. The new elements are products $\Delta^2 \times I$. There are exactly 4 of these which are glued onto the 4 faces of Δ^3; see Fig. 11. The result is given in Fig. 12.
Depth 2. There are 10 elements of the form $\Delta^1 \times I^2 = I^3$ which are glued in. This is asymmetric (as it should be). Four of the edges are associated to two cubes and two of the edges to only one cube. The latter two edges do not intersect; see Fig. 13.

After the second blow-up, we see that at each vertex there are precisely $2+2+1$ cubes, which effectively replace the vertex by 5 squares which assemble to a K_4; see Fig. 14. If we "straighten out" the polytope and consolidate the cells, we obtain the usual picture of W_4 (see Fig. 15) which we now see is Δ^3 realized inside W_4. Here "straightening out" means that we glue the cells along their common facets and represent the consolidated outer facets as a plane.

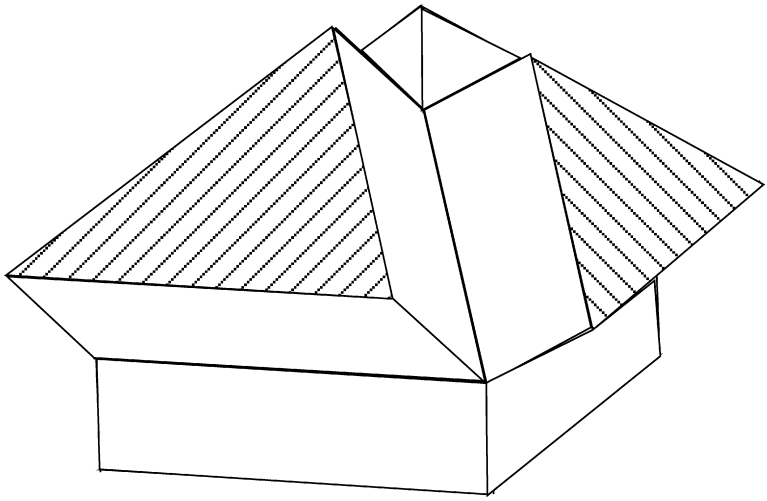

Fig. 12. The result of the first gluing.

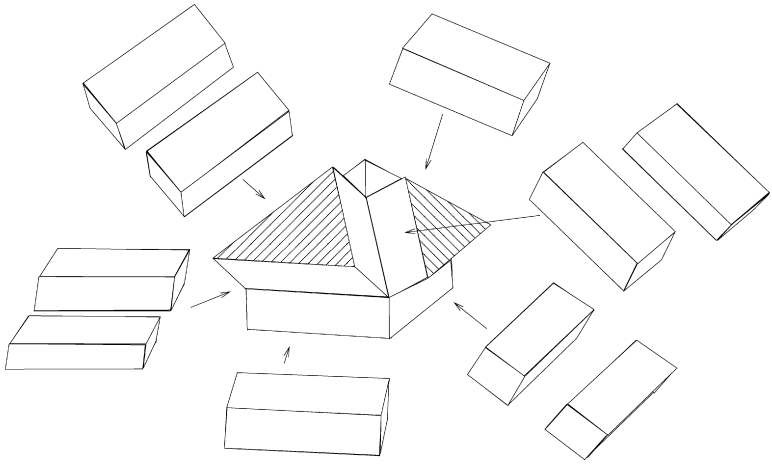

Fig. 13. Step 2: gluing on 10 $\Delta^1 \times I \times I = I^3$s.

Remark B.8. Notice that the procedure above actually gives a PL embedding of W_n into $\mathbb{R}^{n-1}$.

Remark B.9. This iteration can also be understood purely in terms of bracketings instead of trees. We refer the interested reader to [27].

Remark B.10. We can alternatively think of the gluings as a blow-up that comes about by cutting edges to blow up the faces. In the first step, we cut along all the edges and then in the second step, we cut along the four non-special edges. For the purposed of the present paper it was important however, that we have an explicit embedding of the simplex and a retraction to it.

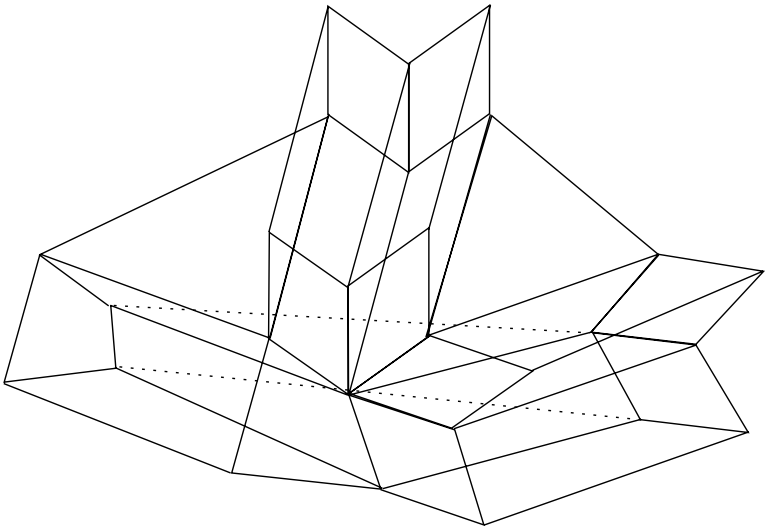

Fig. 14. A vertex after the blow-up.

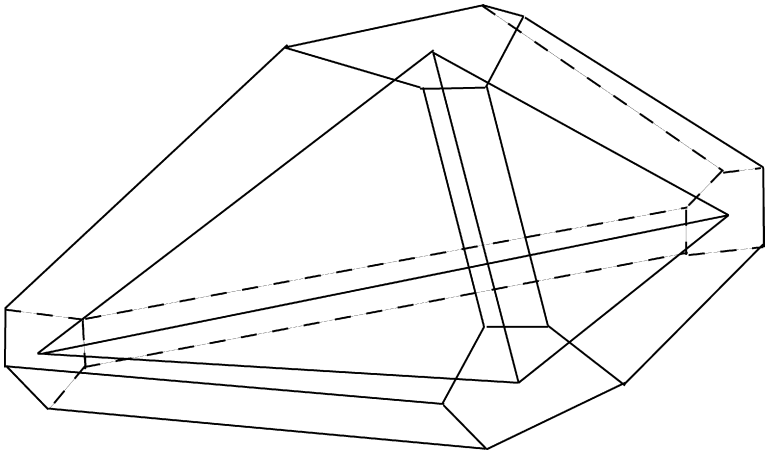

Fig. 15. The simplex Δ^3 inside W_4 after the construction.

References

[1] S. Axelrod, I.M. Singer, Chern–Simons perturbation theory. II, J. Differential Geom. 39 (1) (1994) 173–213.
[2] C. Berger, B. Fresse, Une décomposition prismatique de l'opérade de Barratt–Eccles, C. R. Math. Acad. Sci. Paris 335 (4) (2002) 365–370.
[3] J.M. Boardman, R. Vogt, Homotopy Invariant Algebraic Structures on Topological Spaces, Lecture Notes in Math., vol. 347, Springer-Verlag, Berlin, New York, 1973, x+257 pp.
[4] R. Bott, C. Taubes, On the self-linking of knots. Topology and physics, J. Math. Phys. 35 (10) (1994) 5247–5287.
[5] M.P. Carr, S.L. Devadoss, Coxeter complexes and graph-associahedra, Topology Appl. 153 (12) (2006) 2155–2168.
[6] F. Chapoton, S. Fomin, A. Zelevinsky, Polytopal realizations of generalized associahedra, Canad. Math. Bull. 45 (4) (2002) 537–566, dedicated to Robert V. Moody.
[7] W. Fulton, R. MacPherson, A compactification of configuration spaces, Ann. of Math. (2) 139 (1) (1994) 183–225.

[8] S. Fomin, N. Reading, Generalized cluster complexes and Coxeter combinatorics, Int. Math. Res. Not. 44 (2005) 2709–2757.
[9] M. Gerstenhaber, The cohomology structure of an associative ring, Ann. of Math. 78 (1963) 267–288.
[10] E. Getzler, Cartan homotopy formulas and the Gauss–Manin connection in cyclic homology, in: Quantum Deformations of Algebras and Their Representations, Ramat Gan, 1991/1992; Rehovot, 1991/1992, in: Israel Math. Conf. Proc., vol. 7, Bar-Ilan Univ., Ramat Gan, 1993, pp. 65–78.
[11] M. Haiman, Constructing the associahedron, preprint, 1984, unpublished.
[12] T. Kadeishvili, The structure of the $A(\infty)$-algebra, and the Hochschild and Harrison cohomologies, Trudy Tbiliss. Mat. Inst. Razmadze Akad. Nauk Gruzin. SSR 91 (1988).
[13] R.M. Kaufmann, Operads, moduli of surfaces and quantum algebras, in: N. Tongring, R.C. Penner (Eds.), Woods Hole Mathematics. Perspectives in Mathematics and Physics, in: Ser. Knots Everything, vol. 34, World Scientific, 2004.
[14] R.M. Kaufmann, On several varieties of cacti and their relations, Algebr. Geom. Topol. 5 (2005) 237–300.
[15] R.M. Kaufmann, On spineless cacti, Deligne's conjecture and Connes–Kreimer's Hopf algebra, Topology 46 (1) (2007) 39–88.
[16] R.M. Kaufmann, Moduli space actions on the Hochschild cochain complex I: Cell models, J. Noncommut. Geom. 1 (3) (2007) 333–384.
[17] R.M. Kaufmann, Moduli space actions on the Hochschild cochain complex II: Correlators, J. Noncommut. Geom. 2 (3) (2008) 283–332.
[18] R.M. Kaufmann, Graphs, strings and actions, in: Yu. Tschinkel, Yu. Zarhin (Eds.), Algebra, Arithmetic, and Geometry, vol. II: In Honor of Yu.I. Manin, in: Progr. Math., vol. 270, Birkhäuser Boston, 2010.
[19] R.M. Kaufmann, A proof of a cyclic version of Deligne's conjecture via Cacti, Math. Res. Lett. 15 (5) (2008) 901–921.
[20] R.M. Kaufmann, M. Livernet, R.C. Penner, Arc operads and arc algebras, Geom. Topol. 7 (2003) 511–568.
[21] M. Kontsevich, Operads and motives in deformation quantization, Lett. Math. Phys. 48 (1999) 35–72.
[22] M. Kontsevich, Y. Soibelman, Deformations of algebras over operads and Deligne's conjecture, in: Conférence Moshé Flato 1999, vol. I (Dijon), in: Math. Phys. Stud., vol. 21, Kluwer Academic Publ., Dordrecht, 2000, pp. 255–307.
[23] J.-L. Loday, Realization of the Stasheff polytope, Arch. Math. (Basel) 83 (3) (2004) 267–278.
[24] J.E. McClure, J.H. Smith, H. Jeffrey, A solution of Deligne's Hochschild cohomology conjecture, in: Recent Progress in Homotopy Theory, Baltimore, MD, 2000, in: Contemp. Math., vol. 293, Amer. Math. Soc., Providence, RI, 2002, pp. 153–193.
[25] J.E. McClure, J.H. Smith, H. Jeffrey, Multivariable cochain operations and little n-cubes, J. Amer. Math. Soc. 16 (3) (2003) 681–704.
[26] M. Markl, S. Shnider, J. Stasheff, Operads in Algebra, Topology and Physics, Math. Surveys Monogr., vol. 96, Amer. Math. Soc., Providence, RI, 2002, x+349 pp.
[27] R. Schwell, Operads, polytopes, and the A_∞-Deligne conjecture, Dissertation, University of Connecticut, 2007.
[28] S. Shnider, S. Sternberg, Quantum Groups. From Coalgebras to Drinfel'd Algebras. A Guided Tour, Grad. Texts Math. Phys., vol. II, International Press, Cambridge, MA, 1993, xxii+496 pp.
[29] J.D. Stasheff, On the homotopy associativity of H-spaces, Dissertation, Princeton University, 1961.
[30] J.D. Stasheff, On the homotopy associativity of H-spaces, I, Trans. Amer. Math. Soc. 108 (1963) 275–292.
[31] D. Tamarkin, Another proof of M. Kontsevich formality theorem, preprint, math/9803025;
D. Tamarkin, Formality of chain operad of small squares, Lett. Math. Phys. 66 (1–2) (2003) 65–72.
[32] A.A. Voronov, Homotopy Gerstenhaber algebras, in: Conférence Moshé Flato 1999, vol. II (Dijon), in: Math. Phys. Stud., vol. 22, Kluwer Academic Publ., Dordrecht, 2000, pp. 307–331.
[33] A.A. Voronov, M. Gerstenkhaber, Higher-order operations on the Hochschild complex, Funct. Anal. Appl. 29 (1) (1995) 1–5.